

ABSTRACT

SHIELS, BRIAN PATRICK. Performance Evaluation of Chemical Protective Clothing Materials Under Dynamic Mechanical Deformation. (Under the direction of Juan Paulo Hinestroza)

This thesis presents a comprehensive assessment of testing methodologies currently used for evaluating the performance of protective clothing materials. Special emphasis is placed on highlighting the inadequacy of such test methods and their lack of correlation with real life scenarios which may introduce mechanical deformation.

ASTM F23 standardized rubber sheets were used to evaluate the sorption, permeation and penetration behavior of the samples when exposed to a standardized liquid challenging agent. 2-Chloro-1,3-butadiene (neoprene) was used as the standard chemical protective clothing material and liquid acetone was selected as the standard challenging agent. The dynamic mechanical properties of the samples were assessed via creep and stress relaxation testing techniques using customized submersion clamps.

Quantitative agreement between sorption and permeation experimental data validated the concept that diffusion was the rate-limiting step for the transport of acetone through neoprene rubber. Creep and stress relaxation experiments illustrated a strong time dependency of the storage and loss modulus of the neoprene samples when exposed to the challenging agent. The Young's modulus of the standard material was also found to be a decreasing function of the number of loading-unloading cycles highlighting the effect of mechanical deformation of the barrier properties of protective clothing materials. Potential improvements to existing testing methodologies are proposed and discussed in detail.

**PERFORMANCE EVALUATION OF CHEMICAL PROTECTIVE CLOTHING
MATERIALS UNDER DYNAMIC MECHANICAL DEFORMATION**

by
BRIAN PATRICK SHIELS

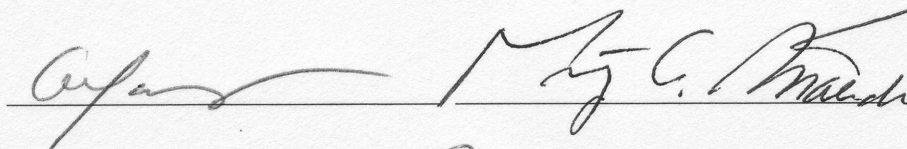
A thesis submitted to the Graduate Faculty of
North Carolina State University
in partial fulfillment of the
requirements for the Degree of
Master of Science

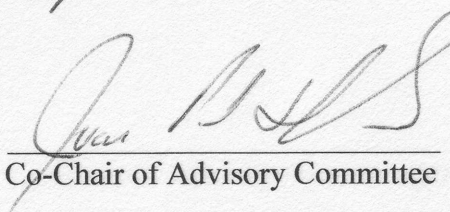
TEXTILE CHEMISTRY

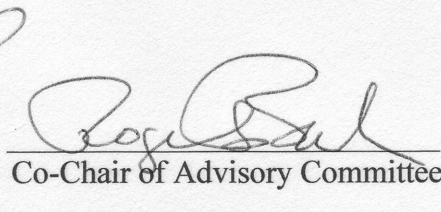
Raleigh

2005

APPROVED BY:




Co-Chair of Advisory Committee


Co-Chair of Advisory Committee

BIOGRAPHY

Brian Patrick Shiels was born November 20, 1981 to Kelly and Dixie Shiels in Charlotte, North Carolina. He grew up in Charlotte and attended South Mecklenburg High School where he graduated in June of 2000.

In August of 2000, Brian moved to Columbia, South Carolina to attend The University of South Carolina. Enrolled in the South Carolina Honors College, Brian studied Chemistry at USC. Outside of class, Brian played for the USC Men's Lacrosse Club. During his sophomore year, Brian began working as an undergraduate research assistant for Dr. Willard S. Moore. Brian's undergraduate thesis is entitled "Chemical Reactions in Submarine Coastal Aquifers". Brian graduated With Honors from the South Carolina Honors College with a Bachelor of Science in Chemistry on December 15, 2003.

A month later, Brian moved to Raleigh, North Carolina to begin work towards a Master of Science in Textile Chemistry at North Carolina State University under the direction of Dr. Juan P. Hinestroza. Brian was privileged to work on one of the first research projects to be funded by the United States Department of Homeland Security. The research group was tasked with developing a chemical/biological resistant firefighter turnout suit. While working towards this project, Brian's personal research revolved around perfecting the ASTM Method F-739. For this, Brian has conducted several experiments to study the various processes that affect permeation of organic solvents through polymer membranes.

Brian will graduate with the Degree of Master of Science on August 9, 2005.

ACKNOWLEDGEMENTS

I would like to gratefully acknowledge my research advisor and mentor, Dr. Juan Hinestroza. Never have I met a man with so much energy and pride in his research. Dr. Hinestroza has been a great model upon which I can build my scientific mind.

I would also like to thank the co-chair of my committee, Dr. Roger Barker, as well as the other members, Dr. Orlando Rojas and Dr. Morteza Khaledi for their guidance and support throughout this process.

I am grateful to all of my fellow graduate students for helping to make light of the stressful moments and sharing so much fun in the less stressful times.

I am especially grateful to my best friend, Amy Waleski. She has been there for me every step of the way with a kind word of encouragement. She has continued to truly be my better half and is always the one who has brightened my day when the stresses of graduate school got me down.

Last, yet most importantly, I would like to thank my family. They have provided never-ending support; often financially, always emotionally. As long as I can remember my family has driven me to excel in all of my endeavors. From helping me with my first ever homework assignment to reassuring me that I will, in fact, finish this thesis. My family has always had a kind word of encouragement, and for that I thank them.

TABLE OF CONTENTS

LIST OF FIGURES.....	V
LIST OF TABLES.....	VI
CHAPTER 1: INTRODUCTION	1
1.1 PURPOSE.....	1
1.2 CHALLENGES	1
1.3 RESEARCH OBJECTIVES	2
CHAPTER 2: LITERATURE REVIEW	4
2.1 FUNDAMENTALS	4
2.1.1 Penetration.....	4
2.1.2 Sorption and Diffusion.....	6
2.1.3 Theoretical Framework for Permeation	8
2.2 EXISTING TECHNIQUES IN PENETRATION AND PERMEATION	11
2.2.1 ASTM F-903.....	11
2.2.2 ASTM F-739.....	13
2.2.3 Other Permeation Methods.....	17
2.3 EFFECT OF STRESS ON PERMEATION	18
2.4 PERMEATION OF MIXTURES.....	19
CHAPTER 3: EXPERIMENTAL.....	22
3.1 PENETRATION	22
3.1.1 Materials.....	22
3.1.2 Methods.....	22
3.2 SORPTION	28
3.2.1 Materials.....	28
3.2.2 Methods.....	29
3.3 DYNAMIC MECHANICAL ANALYSIS	30
3.3.1 Materials.....	32
3.3.2 Methods.....	32
3.4 PERMEATION	33
3.4.1 Materials.....	37
3.4.2 Methods.....	40
CHAPTER 4: RESULTS AND DISCUSSION	45
4.1 PENETRATION	45
4.2 SORPTION	51
4.3 DYNAMIC MECHANICAL ANALYSIS	55
4.4 PERMEATION	73
CHAPTER 5: FUTURE WORK.....	78
5.1 PERMEATION UNDER UNIFORM STRESS	78
5.2 TEMPERATURE- AND HUMIDITY-CONTROLLED PERMEATION.....	83
5.3 MULTI-COMPONENT GAS PERMEATION.....	85
5.4 COMBINED PENETRATION/PERMEATION TEST	89
REFERENCES	92

LIST OF FIGURES

Figure 1: ASTM F903 apparatus with neoprene sample in place.....	24
Figure 2: ASTM F903 apparatus with neoprene sample in place. Three pounds of air pressure is applied to the sample in this case.....	25
Figure 3: Custom submersion clamps for DMA experiments	31
Figure 4: Typical ASTM F739 test cell configuration [63].....	34
Figure 5: Modified ASTM F739 permeation cell in rotated position.....	36
Figure 6: Schematic representation of permeation device and analytical system	39
Figure 7: Full infrared spectrum of gaseous acetone (1078ppm) in nitrogen.....	42
Figure 8: Close-up spectra showing linear increase in peak area with increasing acetone concentration.....	43
Figure 9: Degree of deformation resulting from applied pressure during F903 penetration tests.	50
Figure 10: Relative mass uptake of neoprene soaked in acetone.....	54
Figure 11: Creep-recovery experiments for neoprene samples in air.....	58
Figure 12: Close-up of creep-recovery test showing the time dependency of mechanical properties for neoprene samples in air.....	60
Figure 13: Creep-recovery experiments for neoprene samples in air.....	62
Figure 14: Close-up of strain-time plot of neoprene in acetone showing more dramatic change in the mechanical properties of material as a function time.	64
Figure 15: Using strain curves to determine how modulus changes as a function of time.	66
Figure 16: Time dependent nature of sample modulus in air and in acetone as derived from strain curves	67
Figure 17: Storage moduli for neoprene in air and in acetone taken at 1Hz.	69
Figure 18: Loss moduli of neoprene in air and in acetone taken at 1Hz.	70
Figure 19: Ratio of loss moduli for neoprene in air and in acetone ($G''_{air}/G''_{acetone}$).....	72
Figure 20: Permeation of acetone through neoprene.	75
Figure 21: Device for supplying uniform stress upon a rubber sample for permeation testing.....	79
Figure 22: Deformation of body regions under normal use conditions.....	81
Figure 23: Bench-top environmental chamber for temperature/humidity controlled permeation tests.	84
Figure 24: Schematic representation of proposed challenging gas mixing device.....	87
Figure 25: Gas mixing apparatus for creating mixed gaseous challenges for permeation testing.....	88
Figure 26: Schematic drawing of conceptual design for combination penetration/permeation test cell.....	91

LIST OF TABLES

Table 1: Applied pressure values for specific time frames during penetration testing in accordance with ASTM F903 Procedure D.....	27
Table 2: Physical properties of samples for penetration testing	46
Table 3: Results of F903 Penetration tests.....	48
Table 4: Initial physical properties of neoprene samples used in sorption experiments. .	52
Table 5: Initial geometric parameters for neoprene samples used in DMA testing.....	56
Table 6: Physical parameters of neoprene samples used in the permeation analysis.	74
Table 7: Quantification of likely deformations resulting from specific body movements	82

Chapter 1: Introduction

1.1 Purpose

This research work presents a comprehensive assessment of testing methodologies currently used in evaluating the performance of chemical protective clothing materials. Special emphasis was placed on highlighting the inadequacy of such test methods and their lack of correlation with real life scenarios.

It is well determined that barrier materials used in gloves, boots, and other protective clothing face notable deformation in areas surrounding the knees, elbows, and other highly mobile joints in the body [1-3]. Current testing techniques, including ASTM F903 and F739, dictate that a flat specimen will be evaluated in its virgin state. While these testing conditions are aimed at facilitating ease of experimentation, they are in direct contrast with actual use conditions in which chemical protective clothing is subject to notable stresses and deformation.

In addition, several published reports illustrate that the simultaneous presence of external mechanical deformation and organic solvents cause significant swelling of the chemical protective material leading to decreased mechanical and barrier properties.

The inadequacy of existing testing methodologies may mislead the user on the level of protection expected from a material during real life scenarios.

1.2 Challenges

From an experimental perspective, a major challenge in evaluating the true barrier capabilities of protective clothing materials is the monetary expense involved with performing permeation and sorption tests. Perhaps it is for this reason, that many of these

complex interactions are often overlooked in evaluation of chemical protective clothing. The expense of this experimentation is multifold. First, highly specialized and expensive permeation cells need to be used. Secondly, costly analytical techniques are required in order to have high sensitivity at lower concentration levels while maintaining high signal to noise ratios.

Several researchers have studied permeation through non-elongated membranes [4-8]. However, this is not necessarily a representation of real-world application of protective clothing materials. Only few investigators have studied permeation under uniaxial and biaxial elongation [3, 9-11]. Design and fabrication of a device to uniformly elongate the membrane for permeation testing appears to be a major challenge.

Although extensive measures are taken in order to ensure uniform manufacture of these polymer films, it is very difficult to create a perfectly uniform film. Thickness inconsistencies present a challenge in this type of evaluation as it is well documented that permeation breakthrough times are a linear function of the specimen's thickness [12-16].

1.3 Research Objectives

The basic objective of this work is to assess the inadequacy of existing testing methodologies on the performance evaluation of chemical protective materials in representation of real life use conditions. In order to guarantee meaningful comparisons among existing testing methodologies, a standardized ASTM F23 neoprene rubber sample was used. Liquid acetone was chosen as a challenging agent in order to compare the experimental data with an inter-laboratory study coordinated by ASTM in 1999.

Specific objectives of this work include:

1. Determine the sorption behavior of acetone through neoprene.
2. Determine the penetration behavior of acetone through neoprene via ASTM F903-03.
3. Determine breakthrough times as well as steady state permeation rates for acetone through neoprene via ASTM F739-99.
4. Determine the effect of dynamic mechanical deformation on the viscoelastic properties of neoprene.
5. Determine the effect of simultaneous dynamic mechanical deformation and exposure to acetone on the viscoelastic properties and barrier properties of neoprene.

Achievement of these objectives will help to assess the inadequacy of existing testing methodologies in their representation of actual use conditions. By completing the tests as prescribed in the existing standardized methods, a baseline is obtained. However, it is important to explore if and how the mechanical properties of a material change over time with normal use to determine whether evaluation of virgin material is appropriate. Determination of these changes will lead to an assessment of the potential pitfalls of evaluating chemical protective clothing materials as prescribed by the existing standard test methods.

Chapter 2: Literature Review

2.1 Fundamentals

Two main aspects of protection are resistance to penetration and resistance to permeation. Penetration is the simpler of the two and involves bulk failure of the protective material. Unlike penetration, permeation is far more complex and involves a combination of the thermodynamic and kinetic processes of sorption and diffusion. While these two concepts are well defined in the polymer science academic community, a great deal of ambiguity is present in the protective clothing literature when differentiating between penetration and permeation.

2.1.1 Penetration

Penetration is defined by the American Society for Testing and Materials (ASTM) as “the movement of matter through closures, porous material, seams, and pinholes or other imperfections in protective clothing on a non-molecular level” [17]. Such an “imperfection” may be a small tear or a simple pinhole that has developed with use or simply an inconsistency in manufacture.

Various types of protective clothing materials, generically defined as “all-body surface filters which protect the worker from chemicals and aerosols” [18] or “a garment used for the purpose of isolating parts of the body from contact with a potential hazard” [17], have been tested for many years for resistance to penetration by various types of challenge agents.

Several methods have been developed to determine the resistance to penetration by transport of a challenge agent either in bulk liquid or liquid or solid aerosols [18-26].

When small pinholes or pores are present in chemical protective clothing, there is a strong likelihood of bulk penetration of liquids. This bulk liquid transport is complex in that it involves interaction between the liquid and the material (and any ill effects of such interaction) as well as the inherent liquid and material properties (i.e. surface tension of the liquid) [27].

In a study of liquid penetration through barrier materials, Miller found that the surface tension of the liquid and the contact angle between the liquid and material are primary contributors to penetration [28].

A few researchers have begun to develop statistical models to predict penetration of challenge agents through different protective clothing materials. Lee and Obendorf's model, in particular, has shown that when the difference in surface tension (γ_{diff}) of the solid (here, the solid would be the protective polymer membrane) and the liquid (challenge agent) is less than -13mN/m , the protective performance is strictly governed by a repellency mechanism. This repellency mechanism is mainly driven by the polymer-penetrant interactions. Furthermore, when γ_{diff} is greater than -13mN/m , the protective performance is governed by three factors: repellency, wicking, and absorbency mechanisms [27].

Lee and Obendorf's latter model for penetration (P) follows Equation 1, where v is the solid volume fraction, and t is the fabric thickness.

$$P = 18 + 0.24\gamma_{diff} - 30v - 22t - 0.010(\gamma_{diff})^2 \quad (1)$$

All of the predictive models known to the author represent penetration through woven and non-woven textile products. To the author's knowledge, there is no existing predictive model regarding liquid penetration through continuous polymeric films. The fact that penetration through solid polymeric films is typically defect (i.e. a tear or pinhole) driven, a predictive statistical model is effectively impossible to derive.

2.1.2 Sorption and Diffusion

The phenomenon of how liquids permeate through polymers and resins is highly complex and, to date, has not been fully described by any single theoretical framework or mathematical model [29-31]. During the process of liquid permeation through a membrane, the challenge agent must first absorb onto one surface of the barrier material (i.e. the outside of a chemical protective clothing), diffuse through the polymer, then desorb from the other surface (i.e. the inside of a chemical protective clothing) [32, 33]. The rate and extent of each of these three steps is controlled by several factors such as structure of the polymer, structure of the challenge agent, temperature, mechanical stress or deformation, interaction between polymer and challenge agent, pre-contamination of the polymer film, etc. [29, 34].

Most theories of diffusion in isotropic polymer membranes are based on an assumption that the rate of transport through the polymer is directly proportional to a concentration gradient measured normal to the material's surface [35]. This phenomenon is known as Case I or Fickian diffusion. While theories of Fickian diffusion have been thoroughly developed, very seldom does a polymer-solvent (polymer-permeant) system follow them [36, 37]. In a 1946 discussion of the Faraday Society, it was noted that, in

many cases, sharp boundaries existed between the swollen and un-swollen regions of a polymer-permeant system. Several years later Alfey characterized this process as Case II or anomalous diffusion [38, 39].

The actual transport of a permeant into the polymer system can be further broken down into two distinct thermodynamic and kinetic components [40]. The thermodynamic aspect of permeation is usually discussed as solubility (or swelling) and the kinetic component as diffusion. In general, the topic of solubility is discussed in terms of a solubility parameter, in a manner similar to that originally proposed by Hildebrand and later revisited by Dixon-Garrett [6]. The concept of swelling is closely related to solubility; however, the final solution is a solid (or gel), not a liquid. Furthermore, identical solubility parameters are not sufficient for describing swelling. This is because the molecular structure of the permeant molecule must be of small enough size to enter into the lattice network of the polymer film. As the permeant molecule is absorbed into the network, the swelling process begins and the polymer chains assume a more elongated conformation. As this process of elongation progresses, an elastic restrictive force opposes the swelling process. Eventually, when the osmotic pressure, which is driving the swelling, and the restrictive forces are equal, a state of equilibrium is reached [41]. Although Flory's basic theory on the swelling of lightly cross-linked rubber is useful in making some qualitative predictions, it cannot fully account for swelling in semi-crystalline thermoplastic polymers below their glass transition temperature (T_g) [42].

Diffusion of the challenge agent (permeant) into the solid polymer matrix is often described using Fick's laws. Fick's first law describes flux through a surface. This flux is assumed to be related to the concentration gradient measured normal to the surface.

For this relation, the proportionality constant is known as the diffusion coefficient.

Fick's second law provides a relation between a change in concentration as a function of time and a change in flux with respect to the position. This model for Fickian diffusion suggests that the permeant is absorbed at a rate proportional to the square root of time ($t^{1/2}$). One of the major criteria for Fickian diffusion is an instantaneous achievement of equilibrium at the surface following some change in conditions. As this instantaneous achievement of equilibrium cannot occur in a polymer matrix, Fickian diffusion is rarely seen when a liquid is permeating a glassy polymer membrane [43, 44].

There is, in fact, a finite rate at which polymer structures change in response to the stresses imposed on them in the sorption or swelling process. Because this rate is finite, deviations from Fickian diffusion are observed. Because every polymer is unique, these deviations, or non-Fickian diffusion behaviors, are very broad and lead to diverse phenomena that cannot be described or predicted by any single model or theory. One common aspect of non-Fickian diffusion is that the permeant travels through the polymer matrix as a plug with a sharp front, unlike the classical exponential profile [45]. In addition, this transport process is further dependent upon the degree of crystallinity and temperature in crystalline or semi-crystalline polymers [46, 47]. Furthermore, the polymer may show permeant-induced crystallization and orthogonal swelling that makes the process even more complex [48, 49].

2.1.3 Theoretical Framework for Permeation

Throughout the past few decades several attempts have been made to develop one single theoretical framework to describe the permeation process and model non-Fickian

diffusion [29, 50]. Crank's model proposed a history-dependent diffusion coefficient containing a term that instantaneously changed with concentration to an equilibrium value [51]. Although Crank's model was able to predict many aspects of non-Fickian diffusion, it still failed to predict the sharp plug-like front of the migrating permeant. This model did, however, introduce the idea of differential swelling stresses at the boundary due to expansive and compressive forces in the swollen and non-swollen regions of the polymer.

Long and Richman challenged the notion of instantaneous equilibration. Their model assumed that the permeant concentration in outer layers of the polymer film increased with time until eventually reaching an equilibrium point. This work introduced the notion of a gradual relaxation of a physical process rather than a discontinuous change in diffusion coefficient as Crank proposed [52, 53].

Petropoulos and Roussis added to the work of Crank and Long and Richman with two distinct changes. First, they used a term for activity gradient rather than that of concentration. Furthermore, they applied the relaxation term to the entire bulk material, rather than simply outer surface layers [54].

A major advance in predicting non-Fickian diffusion was made by Thomas and Windle in the late 1970s. Their new model was able to account for many of the unique features of non-Fickian diffusion that were being observed experimentally. In the Thomas/Windle model, as a permeant enters the polymer it creates an osmotic pressure. This pressure causes swelling, which in turn, creates more space for additional permeant molecules to diffuse into. The plasticizing effect of the permeant causes a viscous creep in the polymer. This model again affirms that the process is not instantaneous and

suggests an induction period in which this can occur. Although it was a major advance, this model still failed to consider external stress [55, 56].

In fact, only a few researchers have studied the effects of stress on the transport properties of permeants in polymers. Over half a century ago, Treloar observed the effect of tensile stress on the swelling of rubber [57]. Treloar noted that, when strained, rubbers tend to absorb more fluid than the same material that has not been strained [58].

Broutman and Kim observed the diffusion of water in graphite-epoxy tensile bars and noted that, while they had little effect on solubility, stresses of up to 25% of the ultimate stress caused significant increase in diffusion coefficient. Gillat and Broutman reported similar work but used 65% of the ultimate stress [59].

Maron and Broutman measured the diffusion of water near its boiling point into both stressed and unstressed fiberglass and graphite-epoxy composites. Here, they reported that both diffusion coefficient and solubility are enhanced at least to some degree when the material is placed under stress. Again, however, the diffusion coefficient was much more heavily influenced than solubility [40, 60].

Williams observed how transport properties of gases in polymers were changed upon drawing of the polymer. Because of the plastic deformation that resulted from cold drawing, Williams noted that the number of available sorption sites was reduced while the activation energy of diffusion was increased [61]. These changes in the material's properties appear to be a direct result of more uniform alignment of the chains and therefore more dense packing and ordering in the amorphous regions. This enhancement in uniformity results from the drawing process.

Gent and Liu measured sorption of various liquid permeants into cis-polyisoprene threads under varying amounts of strain. Here, they noted that the diffusion coefficient was independent of strain for extensions up to 300%. However, for the same amount of strain, the degree of swelling increased by more than 100% [62]. This data supports Treloar's theory.

2.2 Existing Techniques in Penetration and Permeation

Although there have been several methods proposed for studying resistance to penetration of liquids through chemical protective materials, the most common, as of today, is the ASTM standard test method F903.

As for permeation, there have been several methods accepted by the scientific community such as ASTM F739, the International Organization for Standardization (ISO) 6529, and The British Standard Institution (BSI) EN369. Although the ASTM F739 method is most popular in published work, none of these methods is exclusively used [63]. The Environmental Protection Agency (EPA)'s method 9090 also provides a framework for evaluation of permeation resistance of chemical protective clothing but it provides more qualitative results than the others [64].

2.2.1 ASTM F-903

The ASTM test method F903 was first published in 1984 and subsequently revised in 1987, 1990, 1995, 1996, 1998, twice in 1999, and 2003 by the ASTM F23 committee. The 2003 revision was re-approved by the committee in 2004. It provides specifications for the design of a test cell and for the evaluation and documentation of the

barrier effectiveness of materials used in protective clothing by liquid challenges. This test is designed to evaluate finished items of protective clothing or materials serving as candidates for use in the manufacture of protective clothing. It is simply a qualitative visual assessment for pass or fail of the material [17].

A 57.3-mm diameter test cell is used to expose the sample to the challenge liquid. The cell consists of a chamber for the challenge liquid and a restraining ring which holds the “outside” surface of the specimen in contact with the challenge liquid. The “inside” surface of the specimen is open to the atmosphere and visible through a viewing port for pass/fail assessment. The liquid chamber has a volume of approximately 0.050 L, plus an extended port. The port is designed to provide additional volume so as to keep the challenge liquid in continuous contact with the specimen if the applied pressure distends the specimen outward from the test cell, creating added volume to the chamber [17].

The filler port also serves as the connection for pressurized air, in the case where pressure is to be applied. The test method calls for various pressures and times within which to apply these pressures to the system. There is also an allowance for a custom method to be used by the researcher [17].

Specimens for evaluation consist of either a single layer or a composite of multiple layers, which is representative of an actual protective clothing material or construction with all layers arranged in proper order. In the case where seams will be normally found in the design of the protective clothing, a seam must be placed within the area that is in contact with the challenge liquid. Specimens for the test measure a minimum of 65-mm by 65-mm square [17]. A minimum of three samples are taken

randomly throughout the surface of the protective clothing material [65]. There is no specified preconditioning required of these samples.

In cases where a visual failure is difficult to determine, the standard allows for several methods of enhancing the visibility of the challenge liquid. First a drop of the challenge is to be placed on the normally inside surface of the protective clothing to assess visibility. If the liquid is un-discernable on the inside surface, powder, dyes, or fluorescent tags may be used to enhance visibility [66].

In a practical study, Stull et al. noted that while the ASTM F903 method provides adequate pass/fail results, proper test result interpretation requires an understanding of specific failure modes of the material. Furthermore, they noted the importance of selecting this test method only when appropriate. As the method assesses a material's resistance to liquid penetration only, it should be used when splash protection is desired [67].

It is clearly noted that this test method is to be used only for the evaluation of protective clothing materials for the resistance to penetration. Permeation cannot be detected using this method [17].

2.2.2 ASTM F-739

The ASTM test method F739 was first published in 1981 and subsequently revised in 1985, 1991, 1996, 1998, and twice in 1999 by the ASTM F23 committee. It provides specifications for the design of a test cell and for the evaluation of barrier effectiveness of chemical protective clothing under continuous contact with liquids and gases [63]. Specimens for this test consist of pieces cut from finished items of chemical

protective clothing or materials serving as candidates for the manufacture of chemical protective clothing [64].

A dual chambered test cell, 51-mm in diameter, is used to expose the specimen to the challenge agent. The challenge side of the test cell has a volume of approximately 0.045 L and is equipped with a stoppered port for introduction of the challenge agent. The test can be conducted in closed-top or open-top configurations depending upon whether the researcher wishes to control evaporation of the challenge agent. The collection side of the test cell has a volume of approximately 0.10 L and is equipped with inlet and outlet ports, through which the collection medium is passed. The collection medium is typically gaseous nitrogen or air, but in some cases, liquids have been used [68, 69]. This collection medium can be flowed in one of two configurations: open-loop or closed-loop. In open-loop, the collection medium is continually passed through the system and replaced. Whereas, in the closed-loop system, there is a fixed volume of collection medium that is circulated through the system and monitored for permeant concentration.

In the case of extremely low-volatility challenge agents or challenge agents with low water solubility, such as pesticides, a solid sorbant collection medium has been used [70]. In one instance, silicone rubber sheets have been used because they readily absorb hydrophobic compounds and, in turn, readily desorb them in common solvents [71]. Several other methods that utilize solid collection media have been developed but there has yet to be any evaluation of the accuracy of permeation results when using these methods. Important factors regarding the absorbent capacity and the effect of surface contact have not been appropriately evaluated for these methods [72].

The test method specifies that the test sample be conditioned at ambient conditions before its mass and thickness is measured. Subsequently, the sample is placed between two identical PTFE gaskets, which are clamped between the two glass chambers of the test cell. Once the cell is tightened, the collection side of the test cell is sealed by the protective clothing material and therefore, the collection medium can be controlled and monitored. The test temperature, duration, analytical method, and configuration (open- or closed-loop) is to be reported along with the test results [63].

When evaluating a specific protective clothing material for protection against permeation of a specific challenge agent, breakthrough time (BT) and steady-state permeation rate (SSPR) are the two most common parameters to be measured. The BT is usually reported as the time at which the presence of the challenge chemical is first detected on the inside of the test sample. The BT is highly dependent upon the analytical method used in the test. This dependence drove the F23 committee to specify a normalized breakthrough time. This time is defined as the point at which the flux reaches $0.1\text{mg}/\text{cm}^2/\text{min}$ for open-loop configurations and $0.25\text{mg}/\text{cm}^2/\text{min}$ for closed-loop configurations [63]. The SSPR is defined as the constant rate of permeation that is achieved once all forces affecting permeation have reached equilibrium. ASTM's establishment of these two parameters, BT and SSPR, provides appropriate grounds for quantitative comparison of the protective performance of different chemical protective clothing materials.

Assuming the challenge agent being used is sufficiently volatile, it will evaporate from the inside surface once it has permeated through the membrane. This allows for the use of gaseous collection media. Therefore, the collection medium must be quickly and

efficiently removed from the collection chamber and replenished. If the challenge agent is allowed to build up in the collection chamber without removal, it could potentially saturate the collection medium and even condense in the collection chamber. This can serve to change the concentration gradient across the membrane. Furthermore, saturated or near-saturated collection medium may prevent complete evaporation of the challenge agent from the inner surface of the membrane. Each of these adverse situations can lead to a lower measured permeation rate, and in turn, an overestimation of barrier efficiency. If this goes undetected, a chemical protective clothing material may reach the market and be used with a false perception of protection. To prevent this occurrence, it is imperative to select a collection medium with a high capacity for the given solvent keep the collection flowing at a sufficiently high rate. It has been suggested that the concentration of the challenge agent in the collection medium should be maintained at or below 20% of its saturation concentration [73, 74].

Proper flow rate of the collection medium must be attained in order to maintain the desired concentration levels in the collection side of the test cell. In the 1985 version of ASTM F739, the committee recommended a collection medium flow rate of 0.050 L/min. This flow rate would allow for five volume changes per minute of the standard test cell. The 1991 version of the standard increased this rate and allowed for a range of 0.050 to 0.150 L/min of collection medium. All subsequent revisions have maintained this as an acceptable range. The standard does, however, acknowledge the fact that higher flow rates may be necessary in order to accurately measure permeation rates of certain challenge agents. Special cases may include instances where the challenge agent has a low vapor pressure, or an extremely high permeation rate [64].

Very few studies have been conducted to verify the efficiency of collection medium mixing within the collection chamber, or whether these flow rates are sufficient. Most evaluations of protective clothing materials use a fixed collection medium flow rate, assuming it will effectively remove all of the challenge agent from the inner surface of the material without saturation of the collection medium. In a study of trichloroethylene permeation through Saranex-laminated Tyvek, Stampfer et al. increased the flow rate of the collection medium to stay within detector parameters. It was found that this increased flow rate acted to increase the measured SSPR for this specific challenge/barrier combination [75]. Zellers and Sulewski noted that increased flow rates were needed to measure n-methyl pyrrolidone permeation through natural rubber gloves [76]. Later, the pair discovered that the flow rate must be increased from 0.5 to 3.0 L/min in order to reduce the concentration of NMP in their collection medium (N₂) in order to obtain a true SSPR. In a study of four glove materials and 44 challenge agents, Anna et al. discovered that an increased flow rate was needed in 75% of their experiments in order to obtain a true SSPR [64]. This study also noted an apparent decreasing trend in BT with increased flow rates. Although these studies illustrated the need for verification of flow rate in open-loop tests, no sound predictions have been made regarding which solvent/material pairs may need the increased flow.

2.2.3 Other Permeation Methods

As noted in Chapter One, one of the challenges with conducting a proper ASTM F739 test is that it requires an expensive testing assembly made up of the permeation cell,

analytical instrumentation (typically FTIR or gas chromatograph), some sort of valve system for sampling, as well as an efficient data acquisition system [77].

The gravimetric method has been noted as a sufficient method of obtaining BT and SSPR. In this method, the test cell with challenge agent on one side of a membrane and the other side open, is mounted on a balance. Once the challenge agent diffuses into the membrane, saturates the matrix, and reaches the inside surface it will evaporate into the air. This evaporation leads to an overall drop in mass of the system. The time at which a loss in mass is originally detected will be reported as the BT, and subsequently an SSPR is determined as the test proceeds [7, 78]. While this approach is different than that of ASTM F739, it still requires specialized equipment. It would require a custom cell made of a light-weight chemical resistant material, a method of attaching the test sample, and a balance with appropriate supports for the cell. Further disadvantages of this method include the fact that it is only applicable for volatile solvents. Limited air circulation in ambient laboratory conditions may not efficiently sweep the challenge agent from the inside surface of the material. Furthermore, this method does not allow for analysis of the permeant, which is necessary when conducting studies of mixtures of solvents.

2.3 Effect of Stress on Permeation

Cold drawing of crystalline polymers causes orientation, which can improve the physical and barrier properties of these materials [61]. When a fiber is stretched, the polymer chains tend to adopt more elongated conformations, which can more easily pack together leading to increased crystallinity. In a study where a film of linear low density

polyethylene (LLDPE) was oriented (stretched) biaxially, similar increases in crystalline regions were noted using wide-angle X-ray diffractometry [79].

Wolf et al. have studied the effect of stress on the diffusion, solubility, and swelling of eight solvents on poly aryl ether ether ketone (PEEK) [40]. They found that applied stress greatly increases the rate of diffusion and solubility for all eight solvents. When the applied stress reaches a critical value, the solubility is greatly increased and the time to reach saturation is decreased. For example, the solubility of toluene in semi-crystalline PEEK increased from 9% to nearly 40% under 35 MPa of tensile stress. Also, for a similar membrane 0.25 mm thick, the time to reach saturation was reduced from thousands of hours to less than ten. Although these samples were only stressed uniaxially, this was the first study to associate stress-enhanced solubility and swelling with a critical value dependent upon degree of crystallinity, solvent, and temperature [40].

Lee et al. have studied hydrocarbon permeation of hydrocarbons through biaxially strained butyl rubber membranes [80]. They noted that while BT was directly proportional to the film thickness (which decreases with biaxial strain), the SSPR was dependent upon the change in thickness as well as the degree of deformation. In all cases, they found that biaxial deformation of the membrane led to a decrease in BT and an increase in SSPR.

2.4 Permeation of Mixtures

Most of the basic test methods for permeation of single components can also be used for permeation of mixtures; however, measures must be taken in order to identify how much of which species is permeating, and when. This is necessary because many

membranes are selectively permeable and may allow one or more challenge agents to permeate at different rates [81]. Gas chromatography [82], FTIR or GC-mass spectrography for organics, and atomic absorption for inorganics have been found to be convenient methods of detection when trying to identify and quantify the different permeants [83].

In a study of permeation through a 1.0 mm membrane of high density polyethylene (HDPE), August and Tatzky measured transmission rates of six solvents in an equivolume mixture [84]. For their studies, they used a dual compartment apparatus, in which the compartments were separated by the HDPE membrane. The upper compartment was filled with the mixture of the six solvents. The composition of this mixture was held constant. The permeant vapors were removed from the lower compartment, frozen in a cooling trap, and subsequently analyzed using gas chromatography [85].

Britton et al. estimated the partition coefficients and diffusion coefficients of eight compounds in an HDPE membrane using the ASTM F739 method [86]. The eight compounds were mixed in a solution with equimolar concentrations. Britton used a method of immersing then weighing to estimate the solubility coefficient of the permeants. Park and Nibras have also investigated partition and diffusion coefficients of dilute solutions of volatile organic solvents in HDPE membranes. For their studies, they placed the membranes into a bottle filled with the solution and measured weight gain over time. Partition coefficients were calculated using these weight gain measurements. This work, however, could not determine a relationship between partition and diffusion coefficients with concentration[87].

Nelson et al. performed studies on the permeation of bi-component mixtures through polymeric interfaces [88]. In one experiment, where neoprene's resistance to permeation of a mixture of chloroform and toluene was evaluated, the permeation rates were found to be directly proportional to the relative concentrations of each solvent. In a separate experiment, where a mixture of pentane and tri-chloroethylene permeated a polyethylene glove, a large synergism was observed. Instances such as this, where the permeation rate of a mixture exceeds the sum of its parts illustrates the difficulty in accurately predicting the permeation behavior of mixtures.

Hinestroza et al. have since developed a novel device for analysis of solvent permeation under precisely controlled biaxial deformation [3]. In their studies, they have observed that the SSPR of acetone flux through polyisoprene-carbon black membranes increased by 100% when uniaxially stretched to 40% elongation. Furthermore, when the same membrane was stretched biaxially (40% by 40%), the SSPR of acetone flux decreased by 25% [3].

In a more recent study by Hinestroza and De Kee, they observed similar effects with elongated geomembranes made of LLDPE. In this investigation, they challenged the membranes with methylene chloride and trichloroethylene, as well as mixtures thereof. In all cases, stress-enhanced transport was evidenced by reduction in BT by 38-45% and an increase in SSPR by 300-400% [89]. Again, a synergy was observed in the permeation rates of the mixtures.

Chapter 3: Experimental

3.1 Penetration

In order to evaluate resistance to penetration by the liquid challenge agent, ASTM method F903 [17] was employed with some modifications that will be explained herein.

3.1.1 Materials

ASTM F23 Certified neoprene rubber was obtained from Reeves Brothers, Inc., located in Spartanburg, SC. One linear yard of neoprene was supplied on a roll and used without any further treatment [63].

The liquid challenge agent for all penetration tests was 99.7% pure acetone (CAS: 67-64-1) purchased from Fisher Chemical (Fair Lawn, NJ). The acetone was received as a bulk liquid and used without any further treatment.

Mass measurements were performed using a Mettler (Switzerland) PM480 DeltaRange analytical balance.

Applied pressure (where applicable) was introduced using building-supplied high-pressure air without further filtration or purification. Pressure was controlled with regulators incorporated in the penetration testing device.

3.1.2 Methods

A total of thirteen neoprene samples were evaluated for penetration resistance of liquid acetone. Each sample, cut randomly from the supplied neoprene sheet using a template, consisted of a 2.75 inch by 2.75 inch square.

The thickness of each neoprene sample was measured with a Model II Electronic Thickness Tester from the Thwing-Albert Instrument Company (Philadelphia, PA). The electronic thickness tester reported thicknesses to the nearest 0.000001 millimeter. Each sample was measured in five different locations that would fall within the area of the test cell in contact with the challenge agent. Because thickness was not consistent throughout the sample, and because abnormally thin spots (defects) will drive failure, the lowest thickness value was recorded.

The complete penetration test apparatus, as partially shown in Figure 1 with sample mounted, was constructed by the author using the design specified by ASTM F903 Standard. All parts were constructed of stainless steel with the exception of the test cell body and gasket, which were made of PTFE and expanded PTFE, respectively. The optional transparent cover and screen were not used for these experiments. The absence of this shield allowed the membrane to distend outwards upon application of pressure as shown in Figure 2. This allowance could potentially enhance the effect of any defects (i.e. tears or pinholes) that could result in an overall failure of the material.

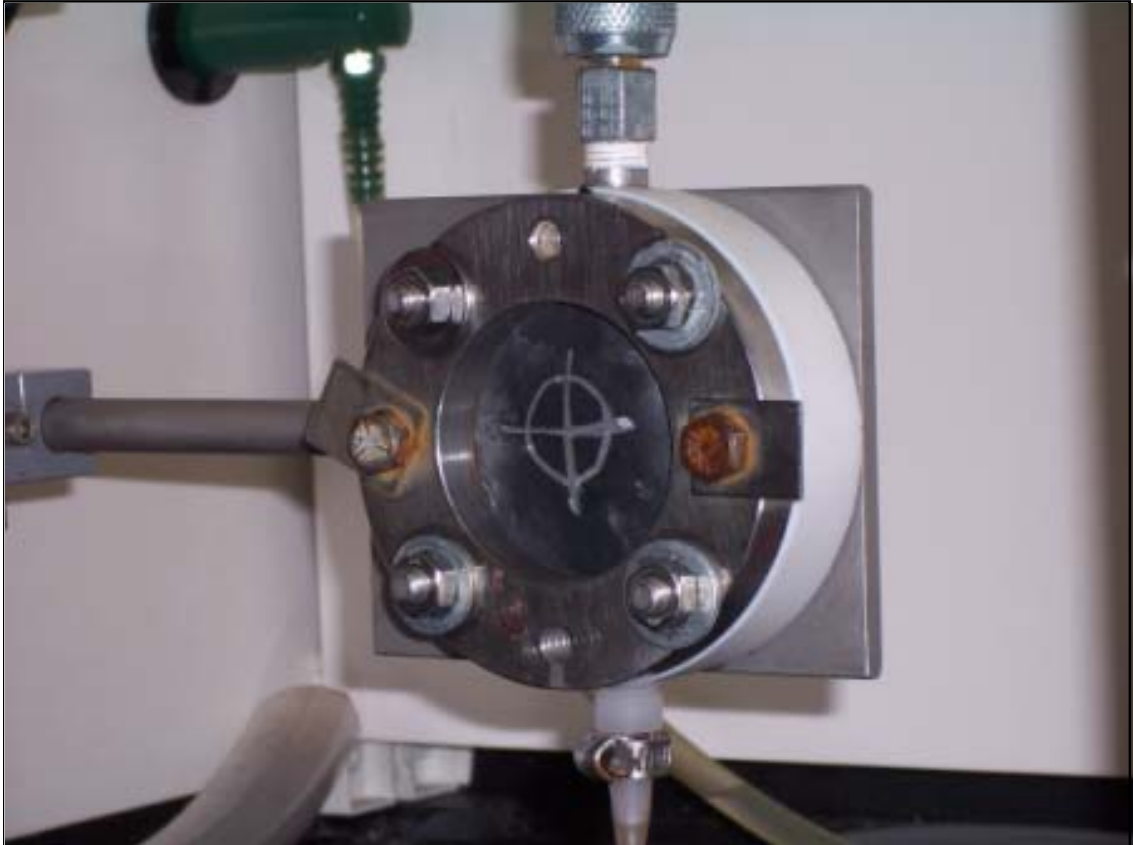


**Figure 1: ASTM F903 apparatus with neoprene sample in place.
No pressure was applied to the sample.**

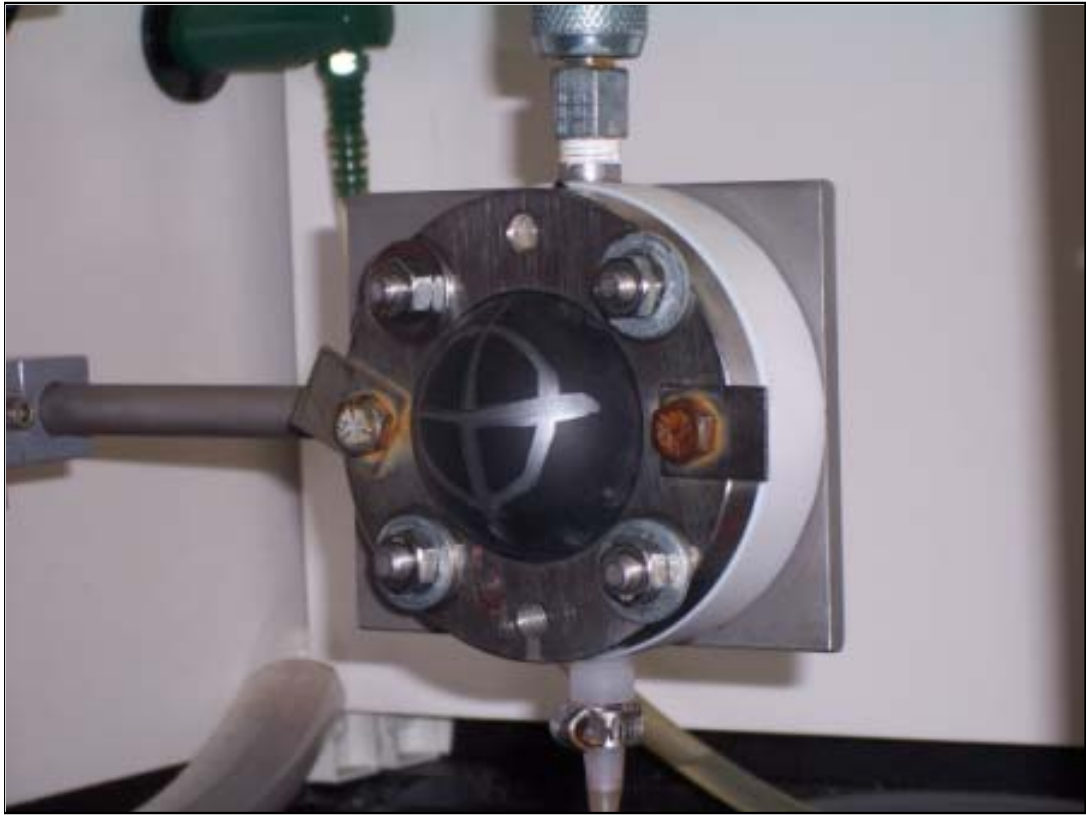


Figure 2: ASTM F903 apparatus with neoprene sample in place. Three pounds of air pressure is applied to the sample in this case. Note the amount of distension in the sample at this pressure.

In order to set visual guidelines for failure, a few drops of acetone were applied to the normally inside surface of the barrier material. Visual analysis of the droplets on the surface of the neoprene was possible. Therefore, none of the suggested indicators was used for these experiments.

The neoprene sample was mounted into the sample cell, and mounted perpendicular to the bench top. A 500mL wash bottle with a finely cut tip was used to introduce the test chemical into the challenge side of the test cell. This method of chemical introduction has been found convenient because it allows for expeditious introduction while allowing the cell to vent (i.e. no pressure builds up prematurely in the cell).

Once the chamber was completely filled with acetone, the timer was started. The procedure for the test consisted of zero psig for the first five minutes, followed by an elevated pressure (in some cases) for the next five minutes, followed by zero psig for the remainder of the test. The total time for the test was 60 minutes. The elevated pressures used in this study are described in Table 1. As these are unique times and pressures values, the exact procedure used would be described by ASTM F903 as “Procedure D” [17]. These pressure values were used in procedures for three replicates of each sample. An attempt was made to evaluate samples at an elevated pressure of 5 psig but the material failed as the pressure applied was higher than 4 psig. The rate of change of pressure applied to the neoprene samples was never more than 0.5 psig per second.

Table 1: Applied pressure values for specific time frames during penetration testing in accordance with ASTM F903 Procedure D.

Penetration Sample ID	Applied Pressure (psi)		
	0-5 min	5-10 min	10-60 min
1.1	0	0.0	0
1.2	0	0.0	0
1.3	0	0.0	0
2.1	0	1.0	0
2.2	0	1.0	0
2.3	0	1.0	0
3.1	0	2.0	0
3.2	0	2.0	0
3.3	0	2.0	0
4.1	0	3.0	0
4.2	0	3.0	0
4.3	0	3.0	0
5	0	<5	N/A

The neoprene sample was observed constantly throughout the duration of the test. Any visible liquid acetone present on the surface of the membrane constituted a failure.

At the conclusion of each test, the sample membrane was removed and any degradation of the membrane was noted. The entire cell assembly was rinsed with water to remove any unseen degradation products that may have been left behind by the membrane. The cell was dried and prepared for subsequent membrane evaluations.

In accordance with the ASTM F903 standards, results for this test are reported simply as pass or fail.

3.2 Sorption

Sorption of acetone into neoprene was determined using a procedure similar to the approach used by Britton [86].

3.2.1 Materials

ASTM certified neoprene samples from the same lot as that used for the penetration tests (Reeves Brothers, Inc.; Spartanburg, SC) were used for sorption analysis.

99.7% pure Acetone from Fisher Chemical (Fair Lawn, NJ) was used as the challenge chemical. Small Petri dishes filled with about 100 mL of acetone were used for immersion of the samples.

All mass measurements were made using a Mettler Toledo (Columbus, OH) model AG204 analytical balance.

The thickness of each neoprene sample was measured using a Model II Electronic Thickness Tester from the Thwing-Albert Instrument Company (Philadelphia, PA).

3.2.2 Methods

Specimens for sorption analysis consisted of small rectangles measuring one centimeter by two centimeters. Three replicates were cut using a template for consistency.

The thickness of each neoprene sample was measured to the nearest 0.000001 millimeter. The thickness was measured in eight to ten different locations and the mean thickness was reported along with standard deviation.

The initial mass was recorded for the sample before any contact with the challenge liquid. After being submerged in the acetone, mass measurements were made every minute for the first ten minutes and every five minutes thereafter up to a total of one hour of submersion.

Using forceps to remove samples from the acetone container, the samples were placed between two lint-free wipes very briefly to remove any liquid that remained on the surface. Samples were then expeditiously placed on the analytical balance and their mass was recorded. The samples were quickly replaced in the acetone and the clock restarted.

Mass measurements were recorded until at least three values were within 1% relative standard deviation of each other. Each test was performed for no less than 60 minutes.

The procedure was repeated for three replicates and percent weight gain was plotted against time for analysis.

3.3 Dynamic Mechanical Analysis

A TA Instruments DMA Q800 was used to perform creep and stress relaxation experiments on the neoprene samples before and after exposure to acetone. Customized submersion clamps, shown in Figure 3, were used to uniformly expose the neoprene samples to liquid acetone.

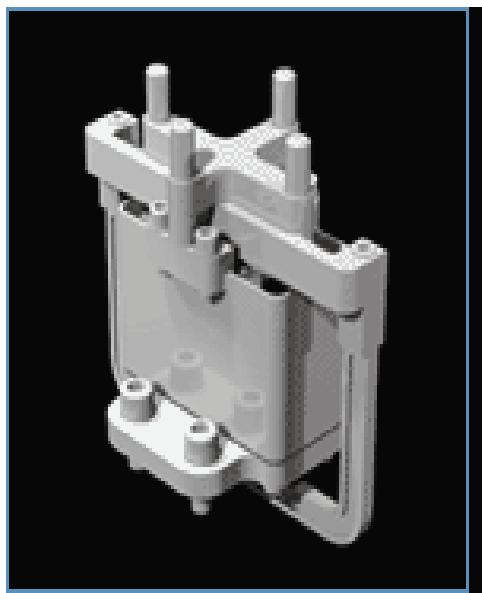


Figure 3: Custom submersion clamps for DMA experiments

3.3.1 Materials

Neoprene from the same lot as that used in the penetration and permeation tests (Reeves Brothers, Inc.; Spartanburg, SC) was used for the DMA testing.

Atmospheric laboratory air was used for “in-air” tests while 99.7% pure Acetone from Fisher Chemical (Fair Lawn, NJ) was used as the challenge chemical for tests that were conducted with samples immersed in a solution.

3.3.2 Methods

Two types of DMA experiments were run. Creep test (stress relaxation) and a dynamic time sweep. All tests were run at a controlled temperature of 25 degrees centigrade.

In the creep test, a finite stress of 0.1 MPa was instantaneously applied to the sample and held constant for a period of time (ten minutes). At the end of that time the stress was instantaneously removed and the material was allowed to relax for twenty minutes. The resulting changes in strain were measured as a function of time. A total of seven creep-relaxation cycles were applied to each sample. The creep tests were performed on samples in air as well as those submerged in acetone.

In both air and acetone, strain was measured over time. Time-strain curves for the material in air and acetone were used for comparison to evaluate the effect of acetone on the mechanical properties of neoprene.

In the dynamic time sweep, frequency, stress, and temperature were held constant at 1 Hz, 0.1 MPa, and 25 degrees centigrade, respectively. Storage and loss modulus

were measured over time in air and in acetone. Comparisons were made of these results in air and acetone to observe the effects of acetone sorption into the neoprene.

3.4 Permeation

The ASTM standard test method F739 (with some modifications by the author) was used in all permeation tests. The main modifications to the test were in the test cell itself. First, the orientation of the test cell was changed from its typical design, in which the barrier fabric is held upright (perpendicular to the bench top) as illustrated in the standard and in Figure 4.

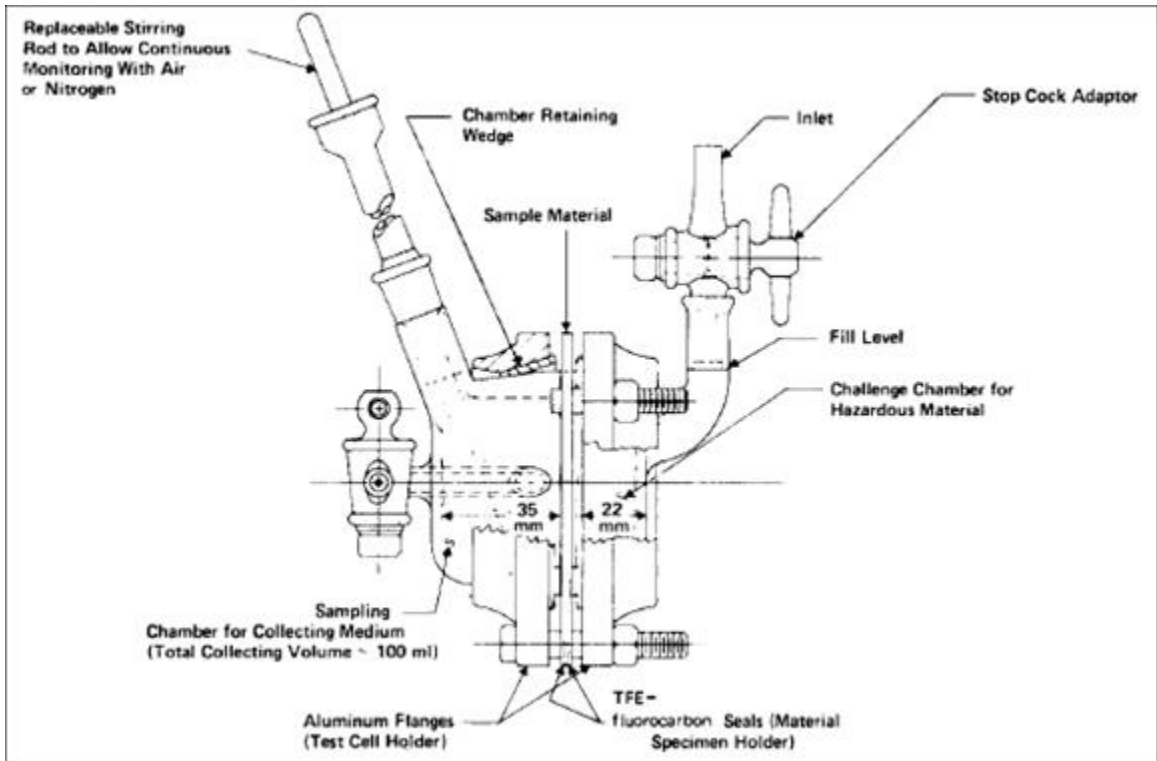


Figure 4: Typical ASTM F739 test cell configuration [63].

For this project, a stage designed by the author was used to hold the cell in a manner rotated 90 degrees from the typical orientation (i.e. membrane is held parallel to the bench top) as seen in Figure 5. Note that the top chamber of the test cell depicted in Figure 5 has two ports where as that of Figure 4 has only one. This was done so that evaluations of both liquid and gaseous permeants could be made using the same experimental setup. Furthermore, this design of the top chamber allows it to be more easily and expeditiously filled with liquid challenge agents.

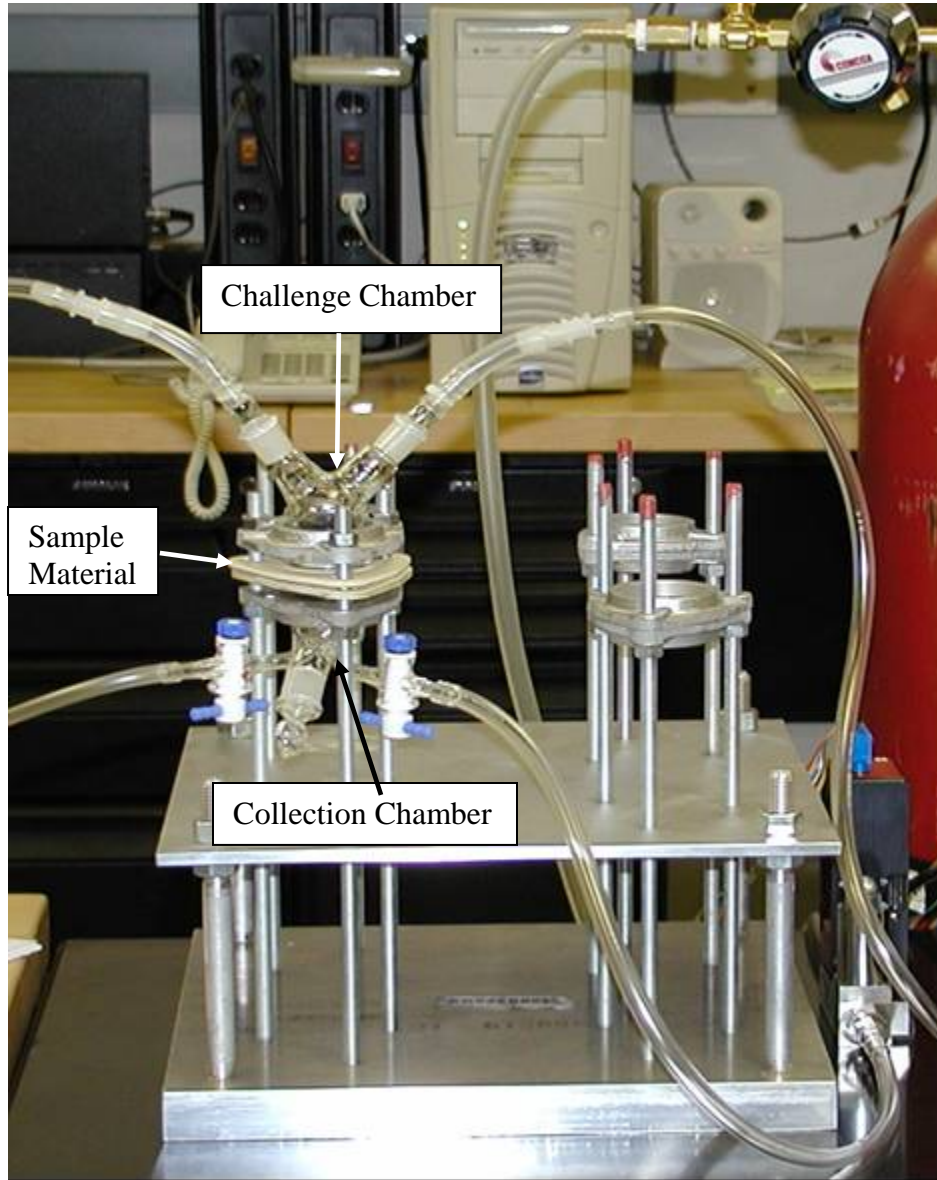


Figure 5: Modified ASTM F739 permeation cell in rotated position.

3.4.1 Materials

Neoprene from the same lot as that used in the penetration and sorption tests (Reeves Brothers, Inc.; Spartanburg, SC) was used for the permeation tests.

99.7% pure acetone from Fisher Chemical (Fair Lawn, NJ) was used as the challenge chemical. The acetone was used as-received with no further purification.

Mass of each sample was measured using a Mettler (Switzerland) PM480 DeltaRange analytical balance.

The permeation cell used was designed by the author and fabricated by the campus glass blower, Janice Singhass (Raleigh, NC). Other than the shape and orientation of the ports in the challenge chamber, the cell meets ASTM design specifications. Standard aluminum flanges, chamber retaining wedges, and PTFE gaskets were used as received from the A.A. Pesce Glass Company (Kennett Square, PA).

All plumbing for the collection medium was made from ¼" Tygon tubing purchased from Cole-Parmer (Vernon Hills, IL).

Industrial nitrogen purchased from Machine and Welding Supply Company (Dunn, NC) was used as the collection medium.

Flow rates of the collection medium were controlled using AFC mass flow controllers model AFC2600D from Aalborg Instruments and Controls, Inc. (Orangeburg, NY). The controllers were interfaced to a command module (model SDPROC-4A1-NA-L-A) also from Aalborg.

Quantitative and qualitative analysis of the collection medium was performed using a Thermo-Nicolet (Madison, WI) Nexus 670 FT-IR e.s.p. in conjunction with its supplied integration software. The FTIR was equipped with a variable path-length IR gas

cell, model 7.2-V, from Infrared Analysis, Inc. (Anaheim, CA). This type of gas cell allowed for continuous sampling of the collection medium throughout the duration of the test.

The entire system is represented in line drawings in Figure 6.

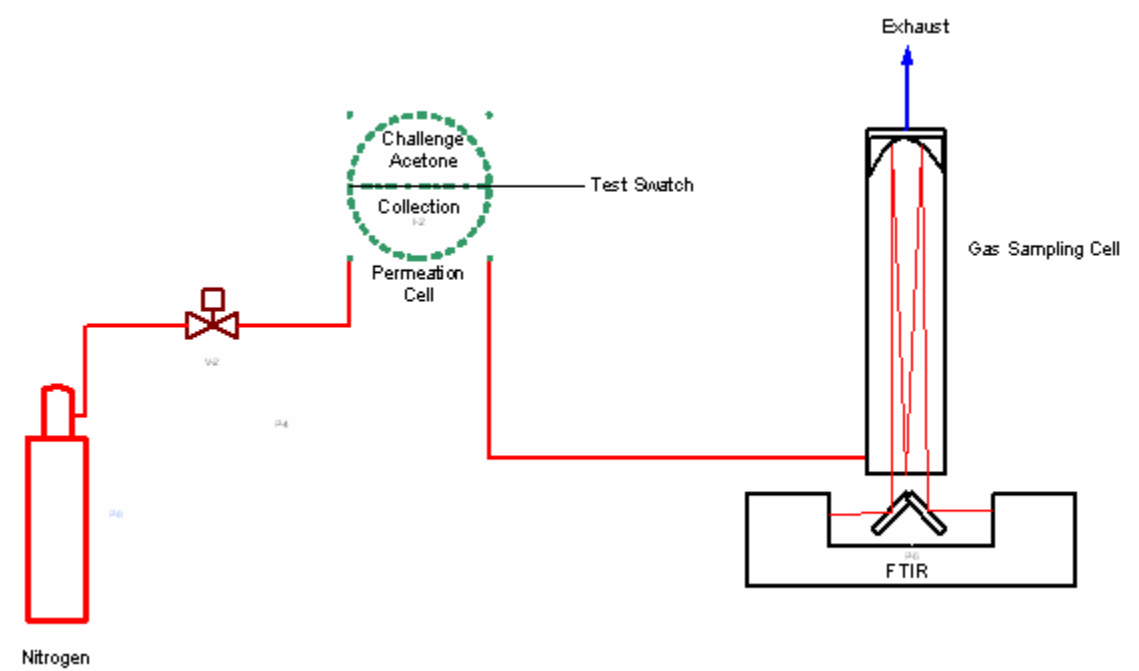


Figure 6: Schematic representation of permeation device and analytical system

3.4.2 Methods

Samples were cut in triplicate from random locations on the neoprene sheet using a two-inch round die punch. This was done in order to ensure uniform size and shape for all samples. The thickness of each neoprene sample was measured to the nearest 0.000001 mm using a Model II Electronic Thickness Tester from the Thwing-Albert Instrument Company (Philadelphia, PA). Mass of each sample was measured using a Mettler (Switzerland) PM480 DeltaRange analytical balance.

The sample was placed between the two PTFE gaskets and the test cell was clamped together. Once properly sealed, flow of the collection medium was commenced at 1.000 standard liters per minute (SLPM) as controlled by mass flow.

Nitrogen was allowed to flow for at least ten minutes to allow for any air or other non-collection medium gases to escape the system. After this period, a background measurement of 32 scans was collected. A new background was recorded for each sample in a similar manner.

The background was saved into the Macros Basic command to be referenced throughout the duration of the test. The Macros was programmed to initiate a new 32-scan analysis every minute for 100 minutes.

The wavenumber region under investigation was $1409.732 \rightarrow 1330.664 \text{ cm}^{-1}$, a documented peak representative of acetone [90]. The Macros was programmed to integrate the area under this peak and subsequently report the peak area into a Microsoft Excel spreadsheet. The full spectrum is illustrated in Figure 7

The test was terminated after 100 data points had been collected (i.e. after 100 minutes). After the test was complete, all remaining acetone was removed from the

challenge chamber with a pipette and disposed of. Any observed gross degradation of the membrane was noted.

Peak area data that was recorded in the spreadsheet was converted first to a parts-per-million (ppm) concentration based on a standard calibration curve performed under identical conditions. Figure 7 shows the entire spectrum while Figure 8 shows linear increase in area under the specified peak with concentration from zero to 1078 ppm.

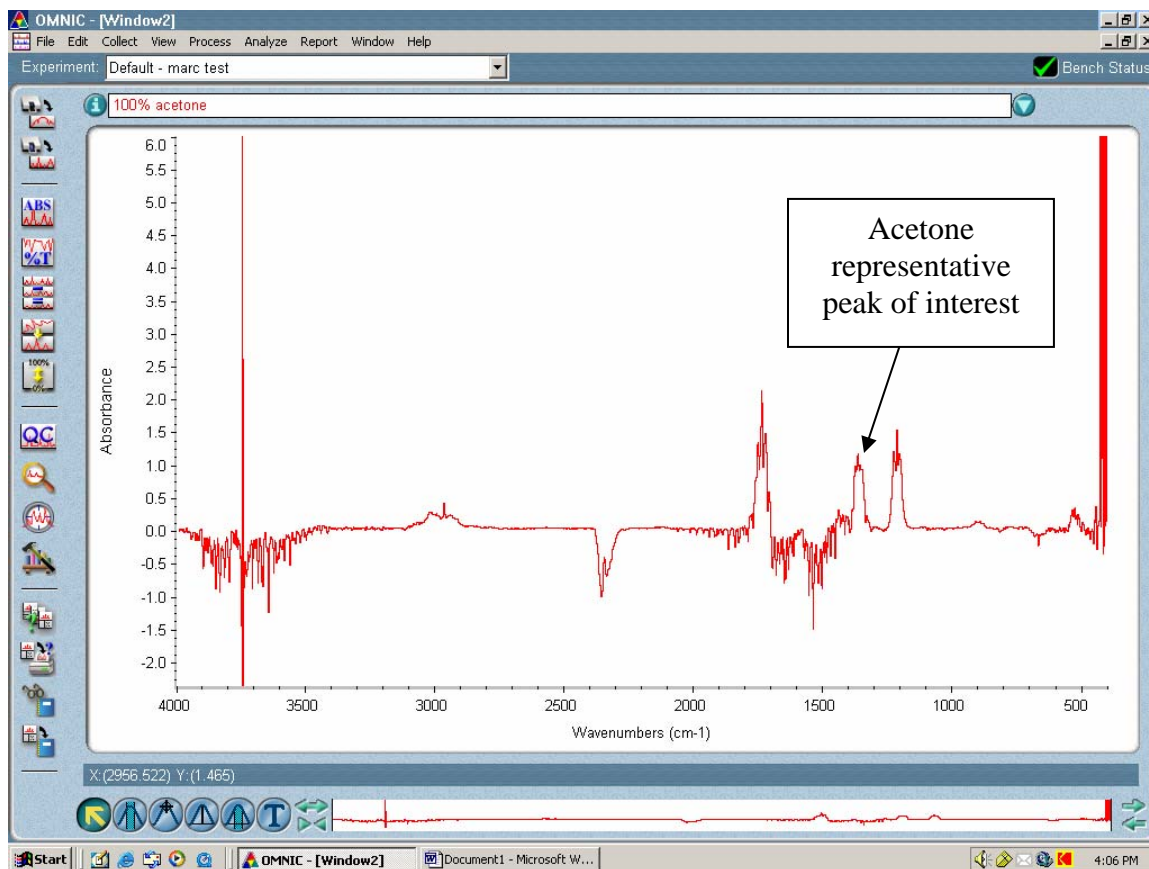


Figure 7: Full infrared spectrum of gaseous acetone (1078ppm) in nitrogen.

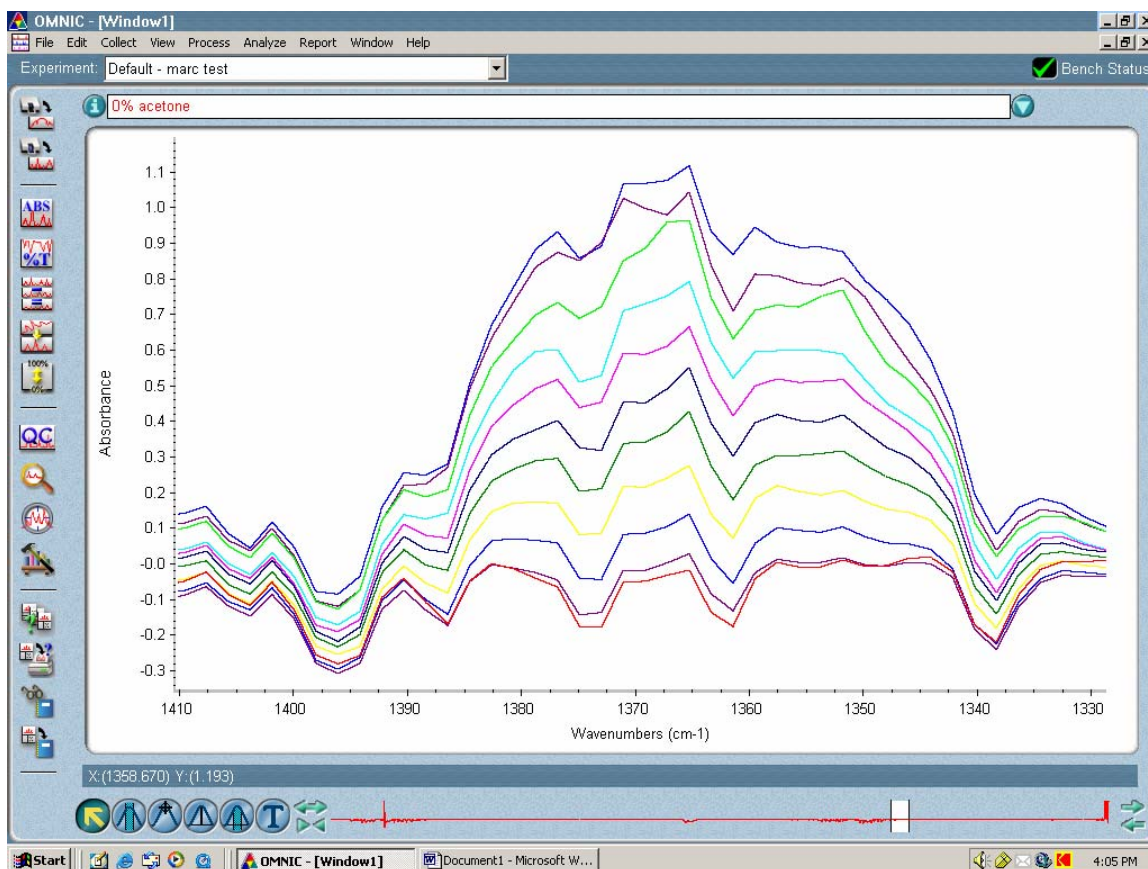


Figure 8: Close-up spectra showing linear increase in peak area with increasing acetone concentration

For simplicity in calculations, the ppm concentration is then converted to $\mu\text{g}/\text{cm}^3$ by Equation 2

$$\frac{\mu\text{g}}{\text{cm}^3} = \frac{(\text{ppm})(\text{MW})(0.001)}{24.45} \quad (2)$$

where MW is the molecular weight of acetone, 58.0798 g/mol.

Given the known membrane area (5.067075 cm^2) for the nominal one-inch cell, the known flow rate of the collection medium ($1000 \text{ cm}^3/\text{min}$), and the measured concentration ($\mu\text{g}/\text{cm}^3$) we can calculate flux in units of $\mu\text{g}/\text{cm}^2/\text{min}$ according to Equation 3.

$$\text{flux} = \frac{(\text{flow rate})(\text{concentration})}{\text{area}} \quad (3)$$

This flux is plotted against time for establishment of BT and SSPR.

Chapter 4: Results and Discussion

4.1 Penetration

A total of ten neoprene samples were evaluated for resistance to bulk, non-molecular penetration of liquid acetone. Before evaluations were conducted, the mass and minimum thickness was recorded for each sample. The physical properties of the samples are listed in Table 2.

Table 2: Physical properties of samples for penetration testing

Penetration Sample ID	Mass (g)	Minimum Thickness (mm)
1.1	2.725	0.39624
1.2	2.857	0.42189
1.3	2.752	0.40818
2.1	2.663	0.40869
2.2	2.828	0.41681
2.3	2.818	0.40869
3.1	2.738	0.40828
3.2	2.716	0.40589
3.3	2.966	0.43713
4.1	2.690	0.39370
4.2	2.739	0.40107
4.3	2.938	0.43688
5	2.785	0.40056

In accordance with the ASTM F903 method, pressure was applied onto the system between the times of five and ten minutes into the test. In all cases, applied pressure caused the sample to distend outward from the sample cell. Pass/Fail results for each sample are listed in Table 3.

Table 3: Results of F903 Penetration tests.

Penetration Sample ID	Elevated Pressure (psi)	Result
1.1	0.0	Pass
1.2	0.0	Pass
1.3	0.0	Pass
2.1	1.0	Pass
2.2	1.0	Pass
2.3	1.0	Pass
3.1	2.0	Pass
3.2	2.0	Pass
3.3	2.0	Pass
4.1	3.0	Pass
4.2	3.0	Pass
4.3	3.0	Pass
5	<5	Fail

Passing results for all samples were expected. In the case of a continuous polymer film, assuming there are no pinhole defects, no bulk non-molecular failure of the material is to be expected.

With added pressure, however, the samples were distended from the sample cell. The membrane had enough strength to maintain structural integrity through three pounds of pressure (psig). However, while increasing pressure upon five psig, the material tore across its entire length. A determination of the degree of deformation is plotted against applied pressure in Figure 9. The structural breakdown of the five psig sample resulted in the only failure of all penetration tests.

Biaxial Deformation of a sample during ASTM F903 tests

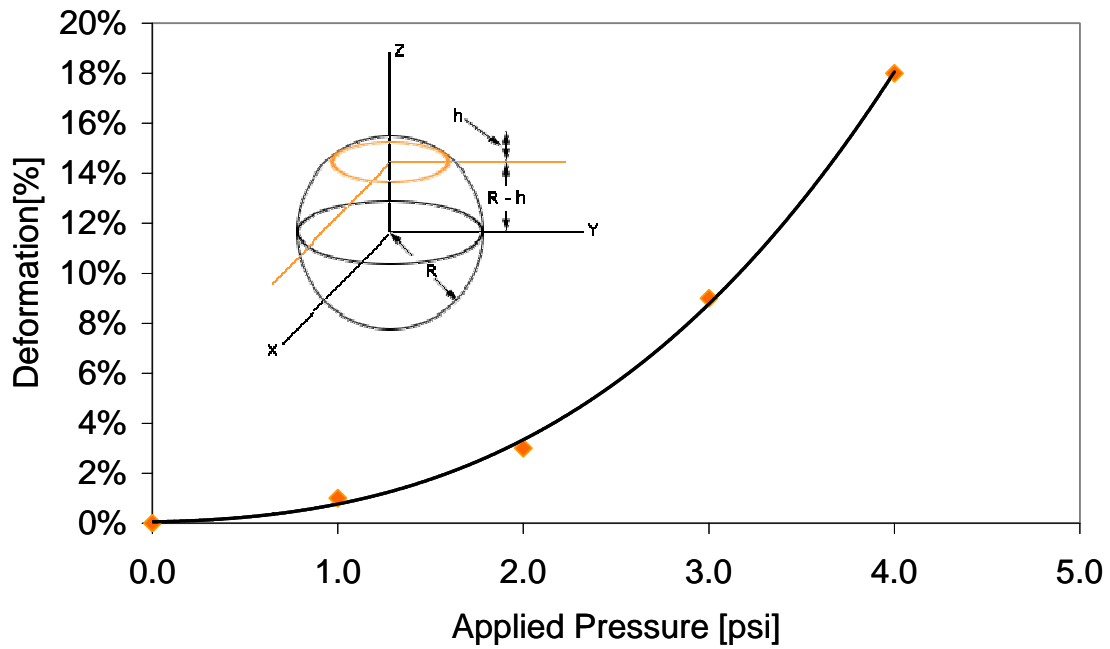


Figure 9: Degree of deformation resulting from applied pressure during F903 penetration tests.

Other than the sample that broke under pressure, there was no obvious degradation of the neoprene in any of the samples. All samples exhibited slightly discolored (white, chalky) spots after the sample was removed from the cell and all acetone was allowed to evaporate from the matrix. This may be caused by the loss of certain fillers in the material, which include carbon black. A loss of carbon black justifies the noticeable loss of color.

As penetration testing is oftentimes used as a preliminary qualification test, these passing results suggest that testing for the material's resistance to permeation on a molecular level will now be appropriate.

4.2 Sorption

To measure the rate of absorption and the time to saturate the matrix, mass uptake of submerged membrane samples was measured at various time intervals. A one centimeter by two centimeter piece of membrane was evaluated in triplicate for sorption.

As done in the evaluation of penetration resistance, the mass and thickness of each sample was measured before any contact with the challenge liquid. The physical properties of each sample are listed in Table 4.

Table 4: Initial physical properties of neoprene samples used in sorption experiments.

Sorption Sample ID	Initial Mass (g)	Thickness (mm)
NDS-1	0.1106	0.399955 ± 0.002185
NDS-2	0.1158	0.425355 ± 0.002477
NDS-3	0.1125	0.419760 ± 0.002152

The mass of the sample was measured every minute for the first ten minutes of immersion in acetone. Subsequently, mass was measured every five minutes, up to one hour of immersion. Because initial masses were not identical, relative mass uptake (in percent) is convenient for comparison purposes. Relative mass uptake measurements are illustrated in Figure 10.

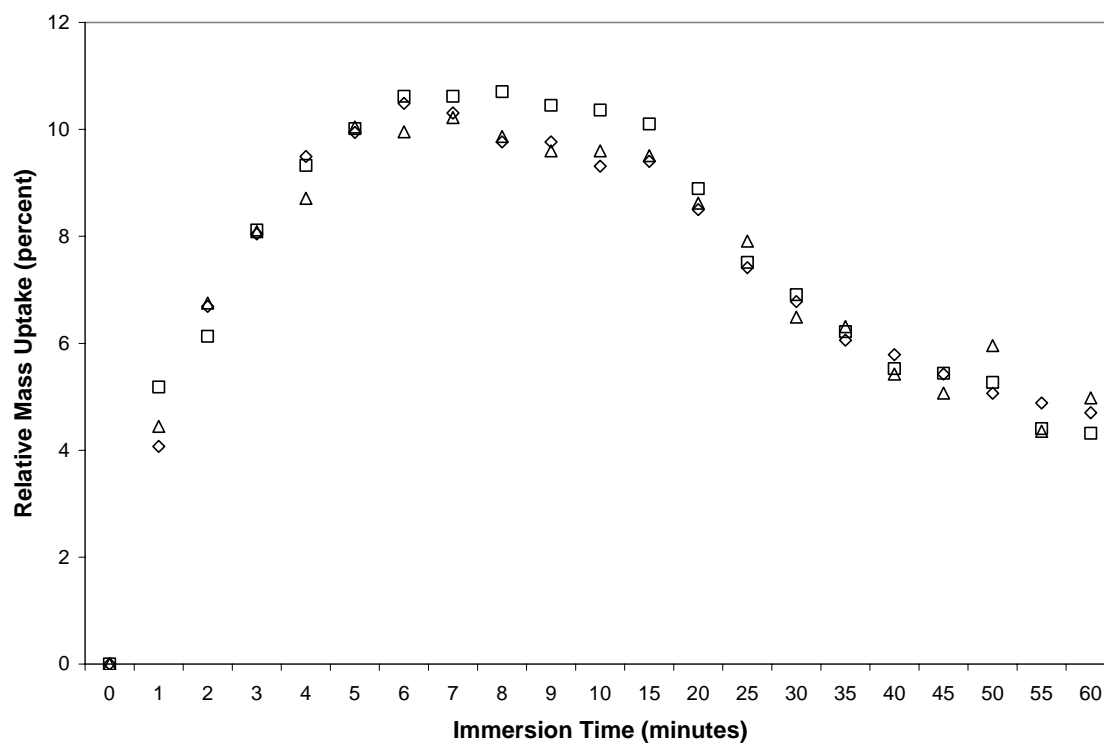


Figure 10: Relative mass uptake of neoprene soaked in acetone. Three replicates are represented.

- Replicate one
- ◇ Replicate two
- △ Replicate three

Initially, the neoprene samples actively absorbed the acetone and linearly gained weight up to a point of maximum sorption. For these samples, the point of maximum sorption is found to be approximately seven to eight minutes.

The drop in mass up take after 20 minutes could be attributed to one or both of two factors. The initial plateau at seven to eight minutes could be representative of a super-saturated condition that eventually equilibrates as evidenced by the drop in mass uptake. More likely however, the drop in mass uptake could be the result of a loss of fillers and plasticizers. Similar to the samples used in the penetration tests, these samples again appeared chalky on their surface after being allowed to dry after testing. Furthermore, the acetone appeared to take on a yellowish tint and appeared to be more viscous after this evaluation. This behavior may suggest the loss of carbon black filler, which would justify decreased relative mass uptake after the point of maximum sorption is reached.

4.3 Dynamic Mechanical Analysis

Initial geometric parameters of each sample were measured and are listed in Table 5. Precise geometries are important for measurements of modulus because small dimensional changes can lead to great changes in modulus [91].

Table 5: Initial geometric parameters for neoprene samples used in DMA testing.

DMA Sample ID	Test	Environment	Length (mm)	Width (mm)	Thickness (mm)
SWD-1	Creep-Recovery	Air	15	8.95	0.43
SWD-2	Creep-Recovery	Acetone	15	8.95	0.43
SWD-3	Dynamic Time Sweep	Air	15	8.62	0.43
SWD-4	Dynamic Time Sweep	Acetone	15	8.62	0.43

Creep and recovery was studied in air to determine a viscoelastic baseline for the material. A series of seven cycles of elongation and recovery were studied with cyclic applications of 0.1 MPa of stress during ten-minute intervals. A plot of strain as a function of time is illustrated in Figure 11. The cyclic stress is superimposed on this plot as well.

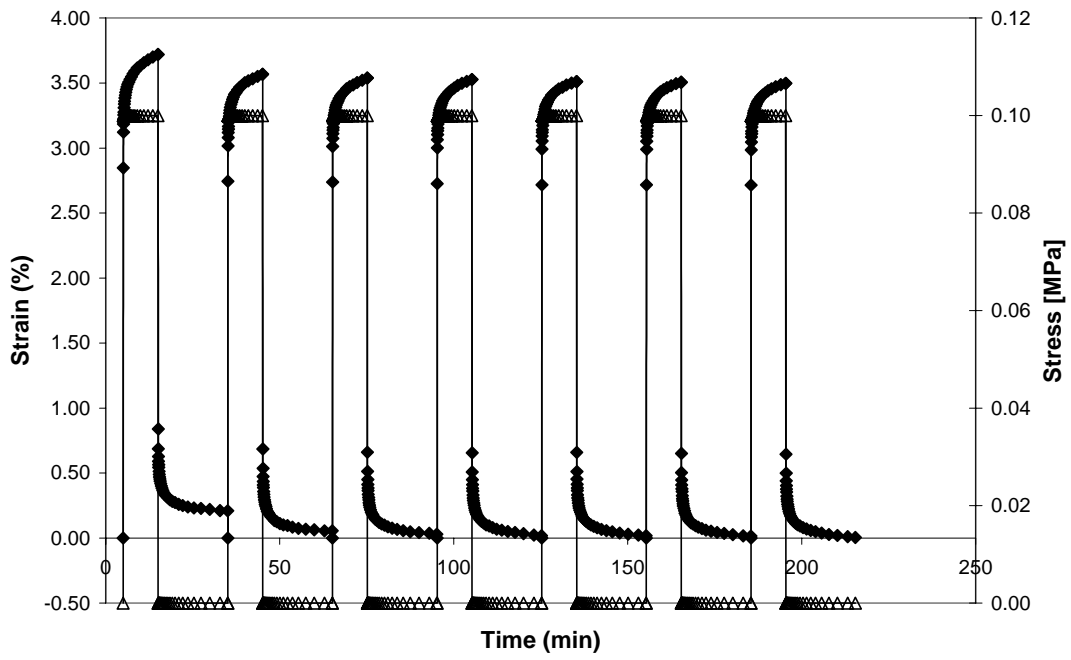


Figure 11: Creep-recovery experiments for neoprene samples in air.

◆ Strain

△ Stress

A closer look at Figure 11 shows that the maximum strain decreases over time with cyclic deformation. In other words, the mechanical properties of the material are time dependent. Figure 12 is presented in a scale that provides a more close-up representation of this change in mechanical properties.

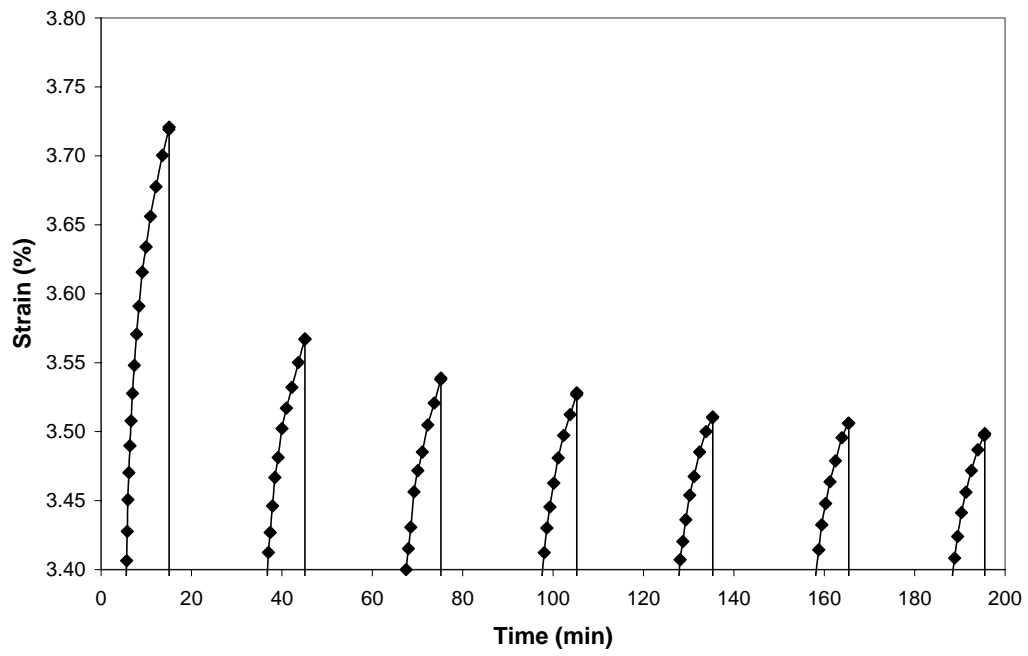


Figure 12: Close-up of creep-recovery test showing the time dependency of mechanical properties for neoprene samples in air.

It is important to note that the changes seen in Figures 11 and 12 are solely the result of mechanical deformation. To this point, no challenging chemical has been introduced to the system. The changes noted in Figure 12 illustrate the need for analysis of chemical protective clothing materials that have been mechanically strained in some fashion, not simply virgin material as is currently dictated by the ASTM F739 standard.

Introduction of a challenge chemical further enhances these effects. Again, neoprene samples were subjected to a series of seven cycles of elongation and recovery with cyclic application of 0.1 MPa of stress. A plot of strain and stress as a function of time is illustrated in Figure 13.

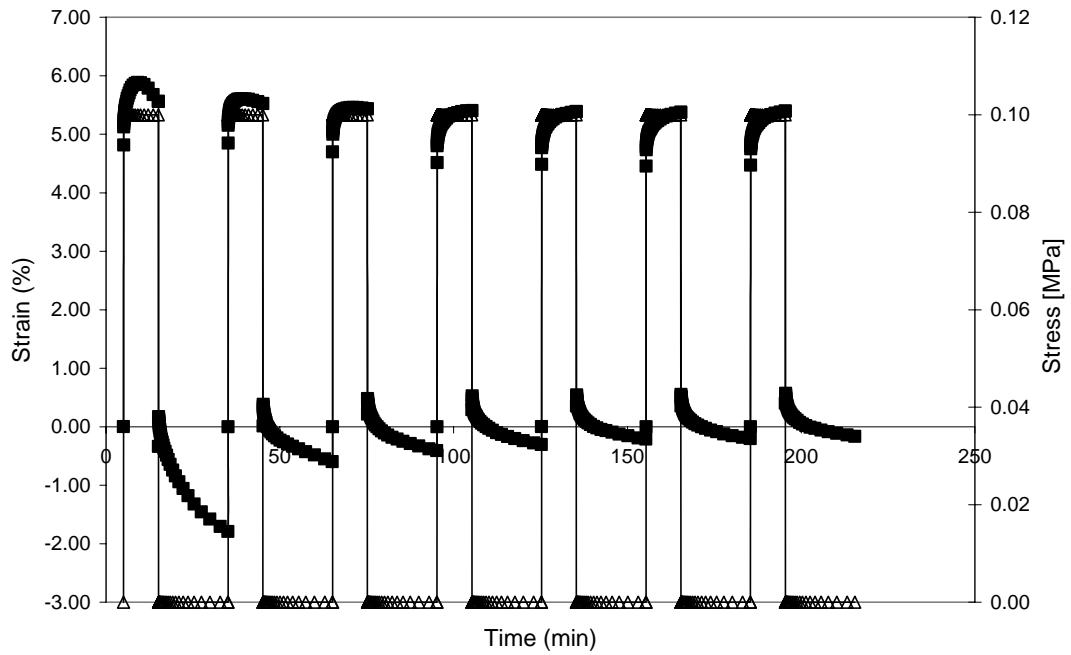


Figure 13: Creep-recovery experiments for neoprene samples in air.

◆ Strain
 △ Stress

Figure 13 shows a markedly increased strain (as a result of equal stress) for the material in acetone versus air. The strain associated with 0.1 MPa of stress for neoprene in acetone is about 50% higher than that when the sample was in air.

The initial anomalies in the stress recovery behavior of neoprene in acetone can be attributed to the sorption of acetone into the polymer matrix.

Upon closer inspection of the strain-time plot, the maximum strain decreases over time as a result of cyclical stress as illustrated in Figure 14. However, in this case, with neoprene submerged in acetone, the difference is about twice as pronounced (0.50% in acetone vs. 0.25% in air).

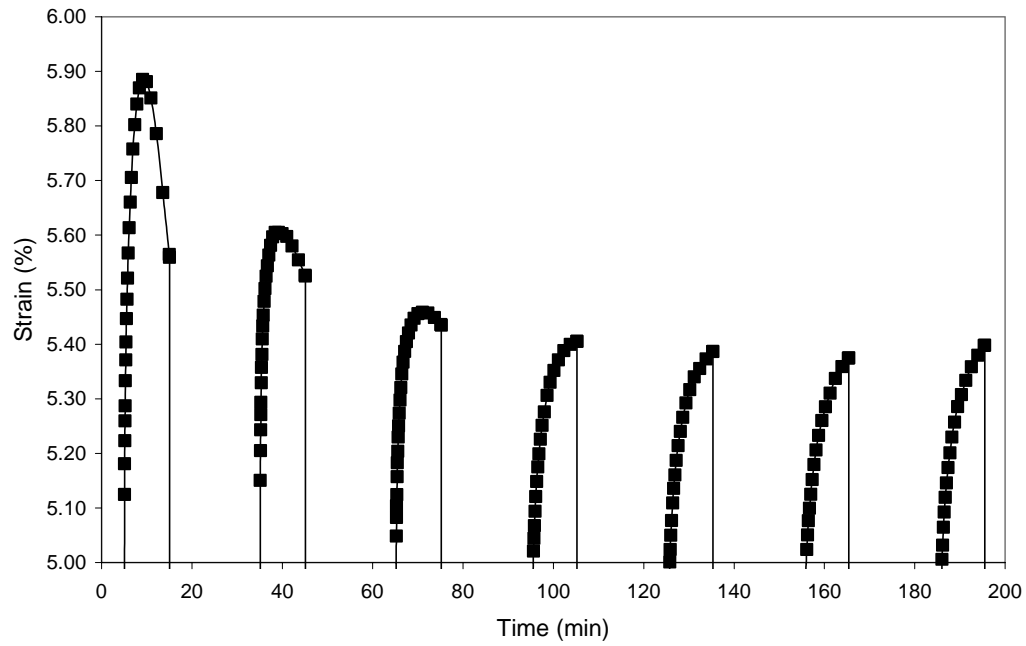


Figure 14: Close-up of strain-time plot of neoprene in acetone showing more dramatic change in the mechanical properties of material as a function time.

Since these changes in mechanical properties are more pronounced when acetone is present, this further demonstrates the need for evaluation of these materials under mechanical deformations representative of actual use conditions.

Careful observation of the upper portion of the strain curves in Figures 11 and 13 provide some insight into the dynamic behavior of the Young's modulus of the material. In Figure 15, a line is superimposed on the linear region of the strain curve and another at the time when the stress is introduced. Based on linear viscoelasticity theory, the line for the linear region is directly proportional to the rate of deformation while the intercept of the two lines is directly proportional to the Young's modulus of the material.

It was observed that this intercept, and therefore the modulus of the material, decreased steadily with time and deformation cycles. This strong time dependence, shown in Figure 16 for samples evaluated both in air and in acetone, illustrates the pitfalls of evaluating a chemical protective clothing material in its virgin state.

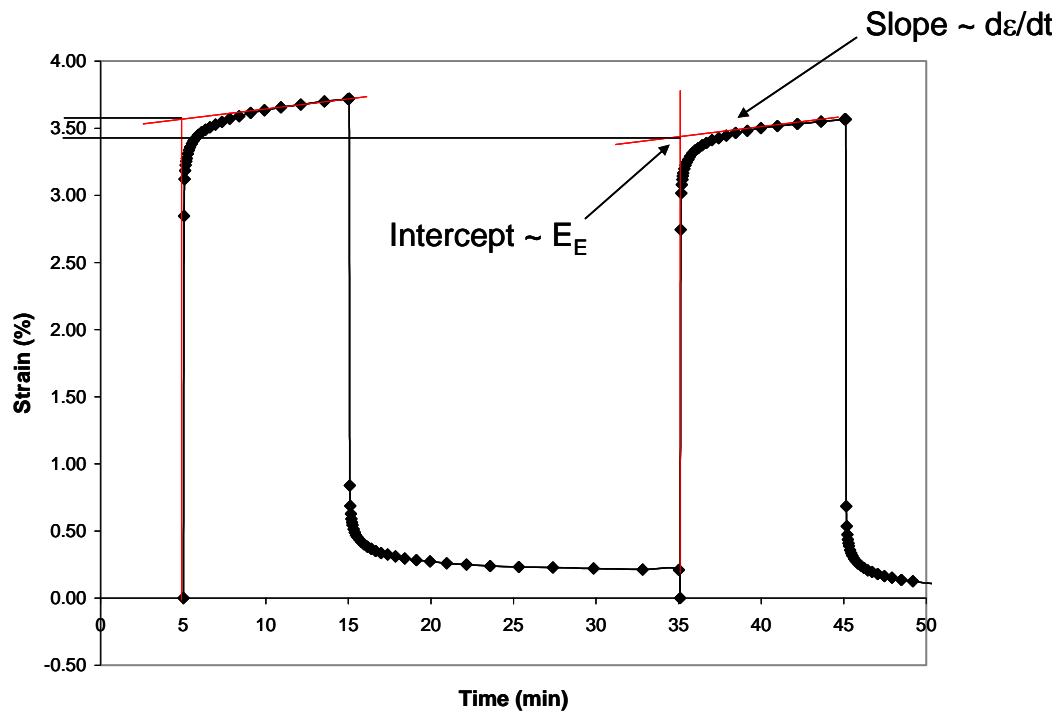


Figure 15: Using strain curves to determine how modulus changes as a function of time.

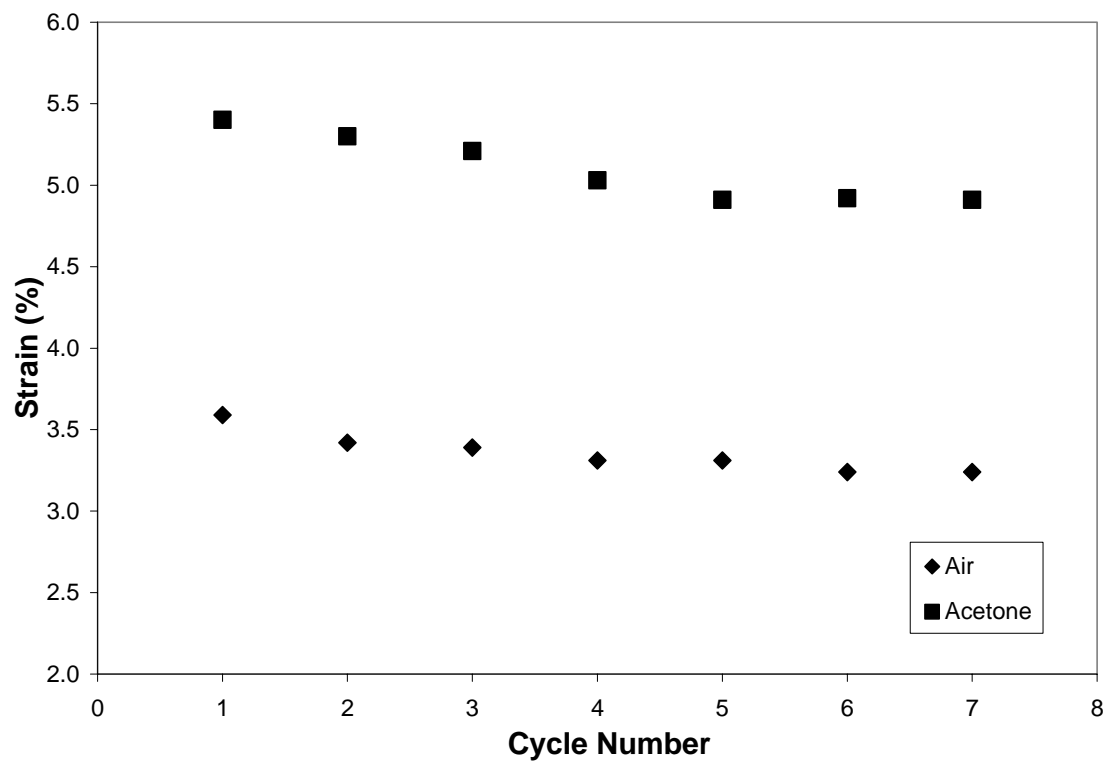


Figure 16: Time dependent nature of sample modulus in air and in acetone as derived from strain curves

The dynamic time sweep provides information regarding the dual nature of a viscoelastic material such as neoprene. The storage modulus (G') describes the solid-like or elastic characteristics of the membrane while the (imaginary) loss modulus (G'') describes the liquid-like or viscous characteristics of the membrane. These two moduli make up the Young's modulus (E) according to Equation 4.

$$E = G' + iG'' \quad (4)$$

The Young's modulus is determined by the slope of the stress-strain curve. In the case of a viscoelastic material, such as neoprene, the majority of Young's modulus is made up of the solid-like G' with a smaller dependence upon liquid-like G'' (i.e. storage modulus is higher than loss modulus). This is evidenced by studying the absolute values in Figures 17 and 19. Nonetheless, both moduli are important and can be used to characterize changes in the material over time and upon addition of acetone.

The elastic or storage modulus is representative of a material's ability to store energy. Figure 17 illustrates the difference in storage modulus of neoprene in air and that of neoprene when exposed to acetone. It was observed that immersion in neoprene resulted in a loss of storage modulus of about 50%.

A drop in the loss modulus for the neoprene sample immersed in acetone is also noted in Figure 18.

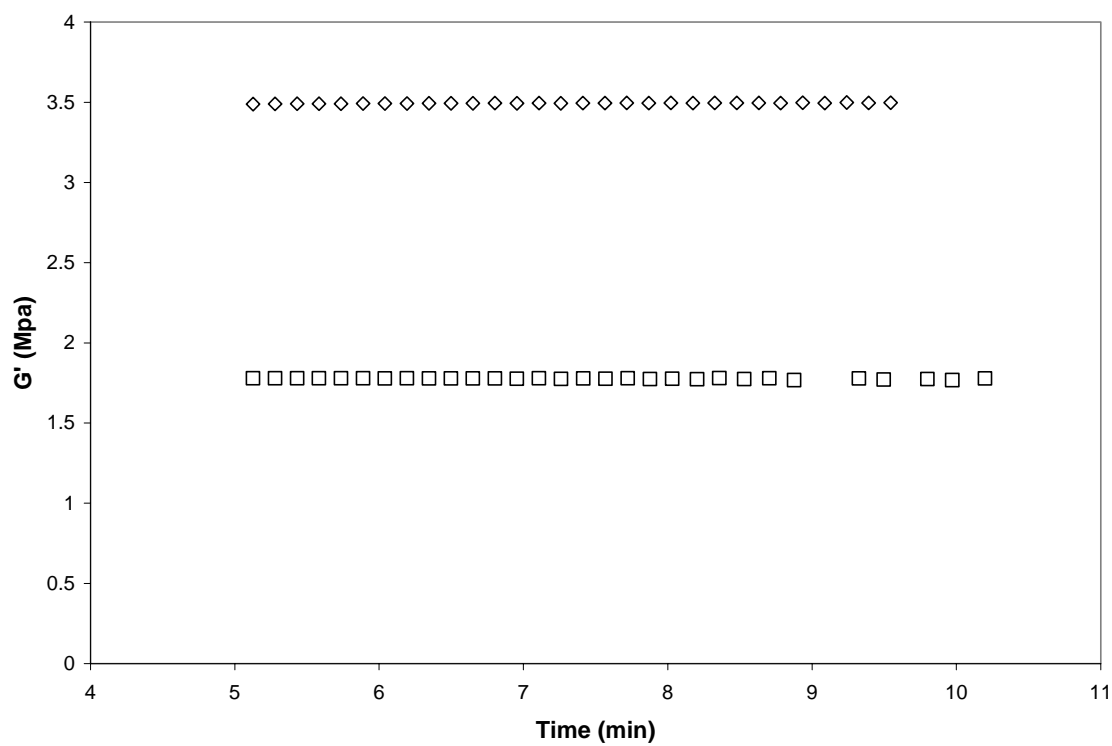


Figure 17: Storage moduli for neoprene in air and in acetone taken at 1Hz.

◇ in air
□ in acetone

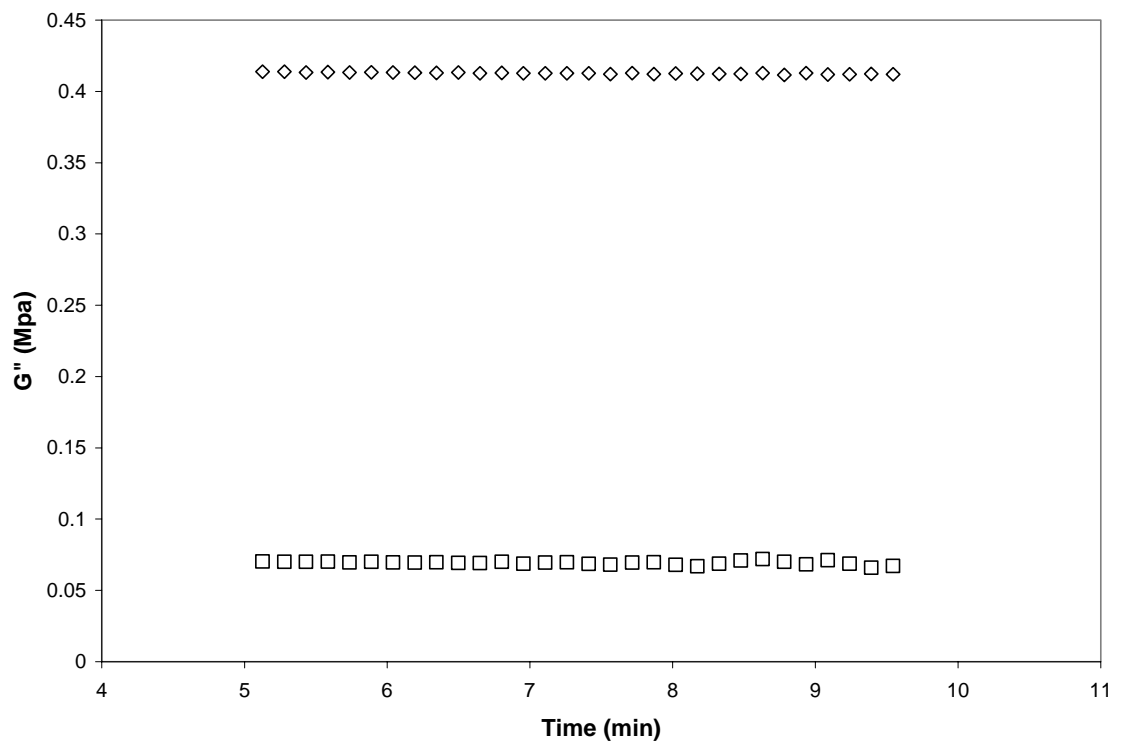


Figure 18: Loss moduli of neoprene in air and in acetone taken at 1Hz.

◇ in air
□ in acetone

Because of the solvent effects on the mechanical properties of the neoprene samples noted in Figures 12 and 14, it is further hypothesized that the loss modulus would drop significantly over time when the sample was immersed in acetone. To assess this drop, the ratio of loss moduli for neoprene in acetone to air ($G''_{\text{air}}/G''_{\text{acetone}}$) was plotted against time in Figure 19. Because there is a positive slope in this graph, it can be concluded that the presence of acetone causes a more dramatic drop in loss modulus than in air alone. In other words, the presence of acetone increases the viscous or liquid-like nature of the polymer. This further demonstrates the effect that sorption of acetone has on the membrane during the permeation process.

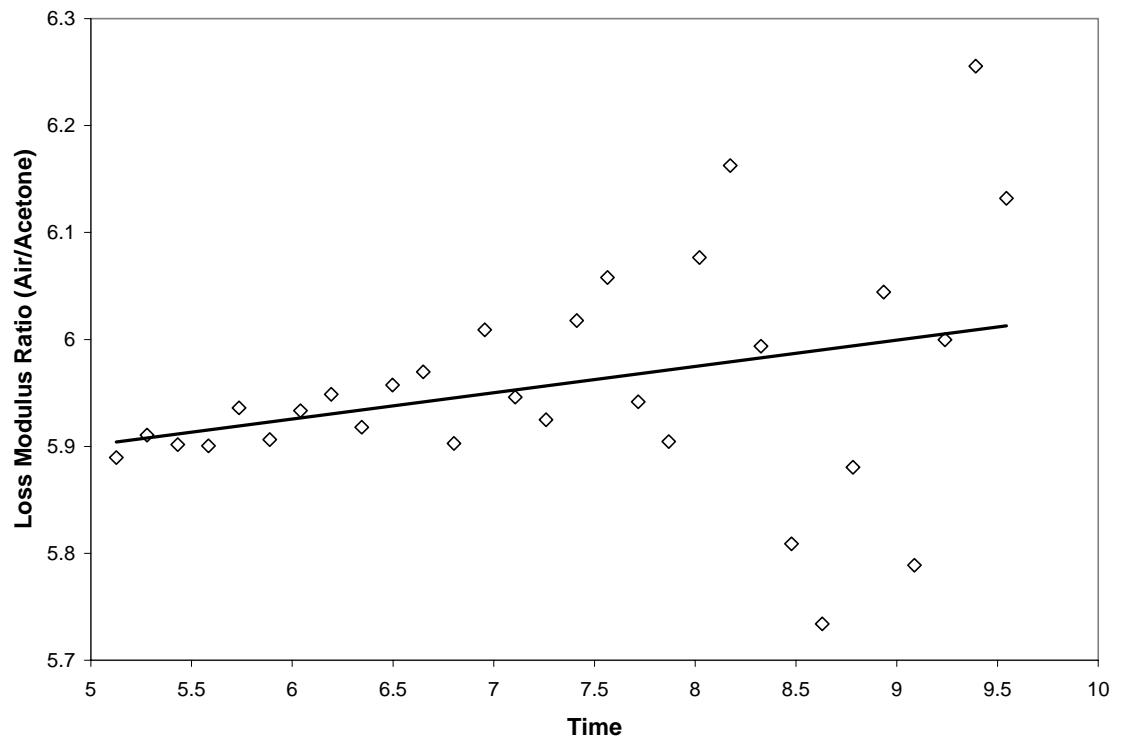


Figure 19: Ratio of loss moduli for neoprene in air and in acetone ($G''_{\text{air}}/G''_{\text{acetone}}$).

In conclusion, DMA data shows several important results. First, the creep-recovery data show that the mechanical properties of the standard material change over time when subjected to cycles of constant stress (i.e. flexing of a gloved hand). This demonstrates the need for evaluations of chemical protective clothing materials to be conducted under mechanical deformation to simulate actual use conditions. Secondly, the dynamic time sweeps showed that acetone significantly affects these changes in mechanical properties, illustrating the compounding effects of mechanical deformation in the presence of solvent.

4.4 Permeation

The physical properties of the samples used for permeation experiments are listed in Table 6. The thickness values illustrated in this table are representative of an average of ten thickness measurements.

Three replicates of acetone permeation through the neoprene sample are illustrated in Figure 20.

Table 6: Physical parameters of neoprene samples used in the permeation analysis.

Permeation Sample ID	Mass (g)	Thickness (mm)
PND-1	1.232	0.446786 ± 0.001292
PND-2	1.204	0.426880 ± 0.001500
PND-3	1.214	0.428980 ± 0.000363

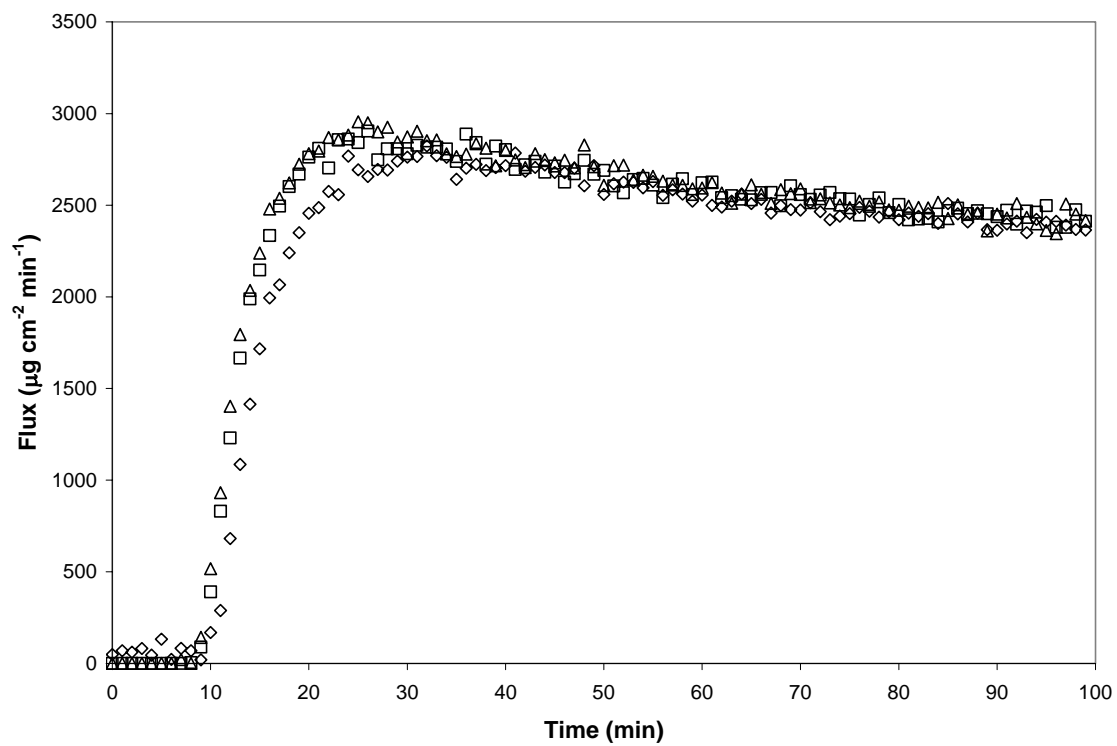


Figure 20: Permeation of acetone through neoprene. Three replicates are represented separately.

- \square Replicate one
- \diamond Replicate two
- \triangle Replicate three

BT was determined to be seven, seven, and eight minutes (\pm one minute), respectively for these tests. This is an expected, yet very important result. In section two of this chapter, it was noted that this neoprene membrane reaches a state of saturation in a range of six to ten minutes. Once the membrane is fully saturated, it is assumed that the next step in the permeation process would be desorption and evaporation from the inside surface. BTs of seven to eight minutes confirm the sorption data suggesting saturation of the membrane at about seven minutes.

SSPR for each of these samples was observed to be around $2500 \mu\text{g}/\text{cm}^2/\text{min}$. The steady-state rate is lower than the local maxima in each case. The maximum permeation rate in each case was between 2750 and $3000 \mu\text{g}/\text{cm}^2/\text{min}$. These observed maxima can be related again to the sorption data. The suggested super-saturation condition could act to overly swell the membrane which would in turn cause an increased rate of permeation. As seen with the sorption data, this elevated rate eventually reaches a lower equilibrium rate (SSPR). This behavior is in agreement with the loss of plasticizer or fillers in the sample during the sorption process.

Furthermore, this observation reiterates Long and Richman's notion [52, 53] that the equilibration is not instantaneous as previously suggested by Crank [51].

The data presented herein supports the hypothesis that existing testing methodologies are inadequate in their representation of real life scenarios. In actual use conditions, chemical protective clothing is repeatedly flexed, stretched, and twisted. Results from DMA experiments, illustrate that the neoprene material studied in this investigation is actually changing as a function of time and use. This time-dependence is only compounded by interaction with challenging agents. Therefore, when a material is

tested in its virgin state, as prescribed in the existing methods, the evaluation fails to determine actual protective performance during real use activities.

Many organizations and governing bodies that use these tests will suggest a preconditioning protocol to represent real use conditions before the material is evaluated. While preconditioning does aid in representation of real use, the test still dictates that the material is tested as a flat swatch of material. However, when the material encounters a chemical challenge, it is most likely being stretched. Therefore, while preconditioning helps to represent wear of the material with use, the test still fails to evaluate the material under mechanical deformation.

This work serves to expose pitfalls in evaluation of immobile virgin chemical protective clothing material for its protective performance. However, much work is still to be done in the way of perfecting these evaluation techniques. Potential improvements to existing test methods as well as possible future evaluation techniques are explained in the next chapter.

Chapter 5: Future work

No single test method is universally accepted or perfectly refined to evaluate the performance of chemical protective clothing. Therefore, the standard test methods are continually evolving in an effort to more accurately represent the true conditions of use for these chemical protective clothing materials. New experiments and test methods will need to be developed in order to optimize the evaluation of potentially life-saving protective garments.

5.1 Permeation under Uniform Stress

Several works have cited the importance of performing permeation tests on materials that have been stressed or elongated [2, 3, 9-11, 89]. However, these investigations have only studied membranes that have been stressed either uniaxially, or biaxially. There is no published research regarding permeation through a uniformly stressed polymer membrane.

An unpublished novel device has been designed and fabricated to introduce uniform stress on a membrane. In this device, shown in Figure 21, a swatch of membrane is mounted into a clamping device that is controlled by a step motor. The device is designed such that when the clamping mechanism is lowered (with membrane attached), the membrane will be pulled uniformly around a ring that is placed on the level of the permeation cell.

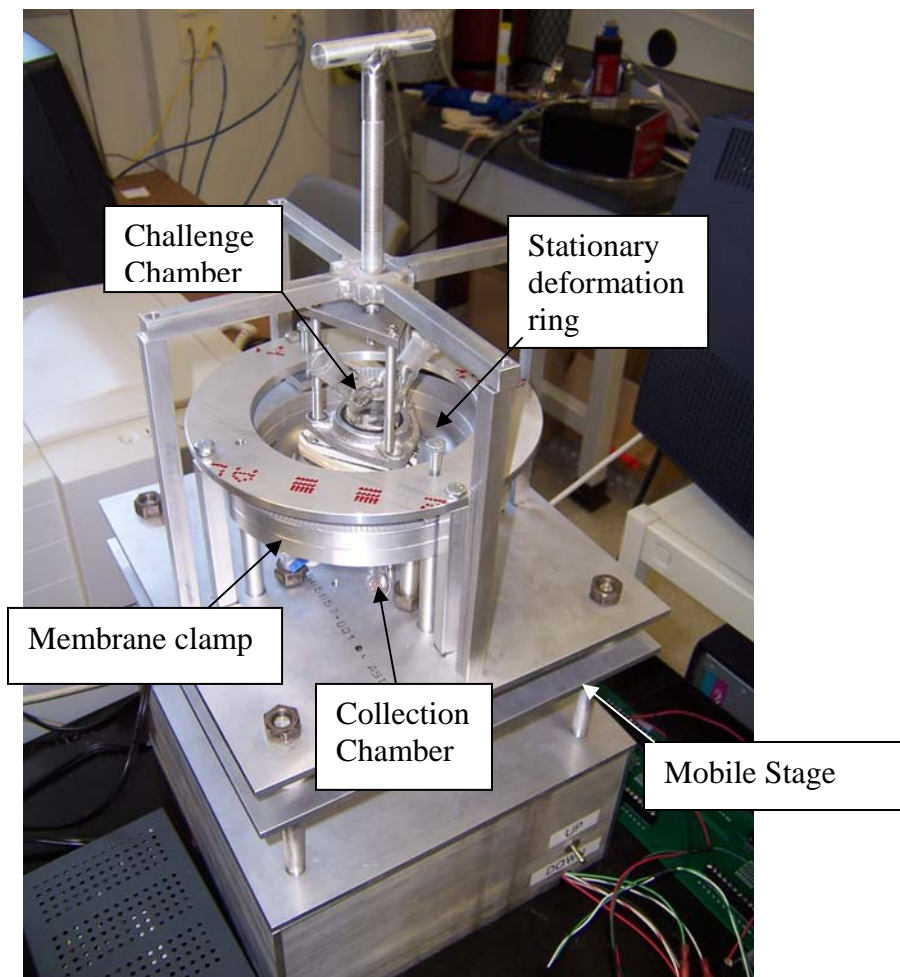


Figure 21: Device for supplying uniform stress upon a rubber sample for permeation testing.

It is thought that a uniform deformation will provide an even closer glimpse into the real-world processes that affect protective clothing materials. When a body part is flexed, the deformation rarely occurs in one or two distinct directions. Figure 22 illustrates how certain parts of clothing are twisted (not perfectly uniaxial or biaxial deformation) under normal use conditions. Table 7 provides quantification for such deformations.

It is the author's speculation that these investigations will lead to similar results found by Hinestroza and others who have performed permeation test on elongated membranes [2, 9, 89, 92].

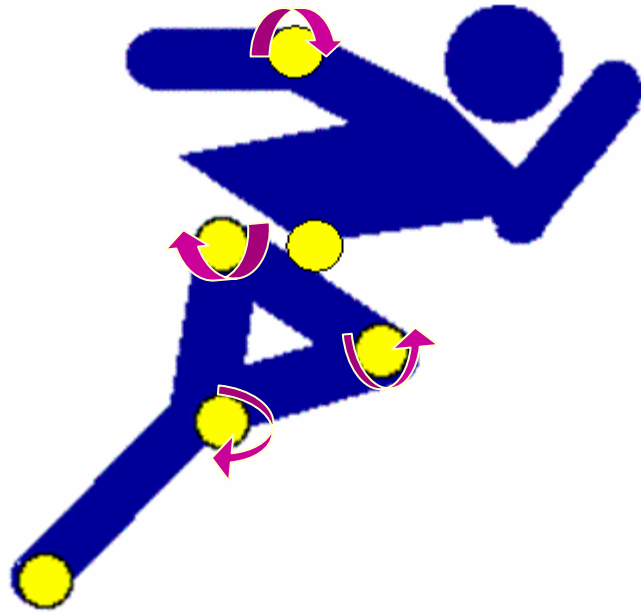


Figure 22: Deformation of body regions under normal use conditions

Table 7: Quantification of likely deformations resulting from specific body movements.

Body Area	Movement	Horizontal %	Vertical %
Back	Straigh to forward arms raised	31-35	
Back	Elbows on the Table	28	
Back	Elbows Bending	14-16	
Back	Shoe-tying	47	
Elbow	Straigh to Full Bending	15-20	50-51
Seat/Hip to Hip	Stand to Sit	15-20	27
Seat/Hip to Hip	Stand to Bend	17-21	34-35
Seat/Crotch	Stand to Sit	35-42	39-40
Seat/Buttocks	Stand to Bend		45
Knee	Stand to Sit	19-21	41-43
Knee	Stand to Deep Bend	28-29	49-52

5.2 Temperature- and Humidity-Controlled Permeation

Some investigators have studied the effects of temperature on permeation resistance. Factors such as, hydrogen bonding, dipole interactions, molecular size, and shape all affect aspects of permeation such as diffusion and solubility. All of these factors are strongly influenced by temperature [93, 94].

Furthermore, humidity is becoming a concern in protective clothing materials. Historically, most tests are conducted with a dry collection medium (in the case of a gaseous collection medium). This is done quite intentionally as one of the restrictions of the test is to maintain a large capacity for solvents in the collection medium. However, knowledge of the swelling or plasticizing effect that water molecules can have on polymers, has driven concern for humidity effects.

In an as-yet unpublished revision of the National Fire Protection Association (NFPA)'s standard on Protective Ensembles for Structural Fire Fighting (NFPA 1971), an optional standard for chemical protection is being included. Within that optional standard, it is specified that all permeation tests are to be conducted at 80% relative humidity.

Because of the newfound need to control both temperature and humidity, the author is currently developing a bench-top environmental chamber, in which precisely controlled permeation experiments can be carried out. The device, pictured in Figure 23, was manufactured by Prism Research Glass (Research Triangle Park, NC) under supervision of the author.



Figure 23: Bench-top environmental chamber for temperature/humidity controlled permeation tests.

Ultraviolet lamps are used in series with controllers to maintain the desired temperature, which is monitored in a feedback loop by a 1/8" thermocouple. In addition, the supply and exhaust lines for the collection medium will be wrapped in thermal tape and controlled in the same feedback loop. Finally, the IR gas sampling cell is being fitted with a custom thermal jacket so that the entire system can be controlled at the precise testing temperature.

In order to introduce humidity into the system, the supply lines for collection medium will be bubbled through distilled water. A humidity probe, installed in the collection chamber of the permeation cell, will provide feedback to a controller that will monitor humidity and change proportions of dry and water-saturated collection medium to maintain the desired testing relative humidity.

This novel device will serve as yet another step towards recreating real-world exposure conditions in the hopes of developing better chemical protective clothing materials.

5.3 Multi-Component Gas Permeation

The cumulative and sometimes synergistic effects of multi-component permeation have been well documented. However, the work that has been done in this area has been concentrated on mixtures of several different liquids. Protection against permeation of hazardous vapors is just as important, if not more so, than protection against liquid permeation. And just as with liquid challenges, vapors will often be encountered as mixtures as opposed to a pure single component. In fact, Earth's atmosphere is composed of a complex mixture of vapors including nitrogen, oxygen, argon, and carbon

dioxide, all of which could potentially enhance, or perhaps inhibit, the permeation of a single hazardous vapor.

To study these conditions, the author has designed and constructed a system to mix up to four gases in precisely controlled proportions. This mixture could now be used as a gaseous challenge agent in the ASTM F739 permeation test. The mixing device, represented schematically in Figure 24 and pictured in Figure 25, consists of four shut-off valves, four mass-flow controllers, four one-way check valves, and a plumbing system to mix the gases downstream.

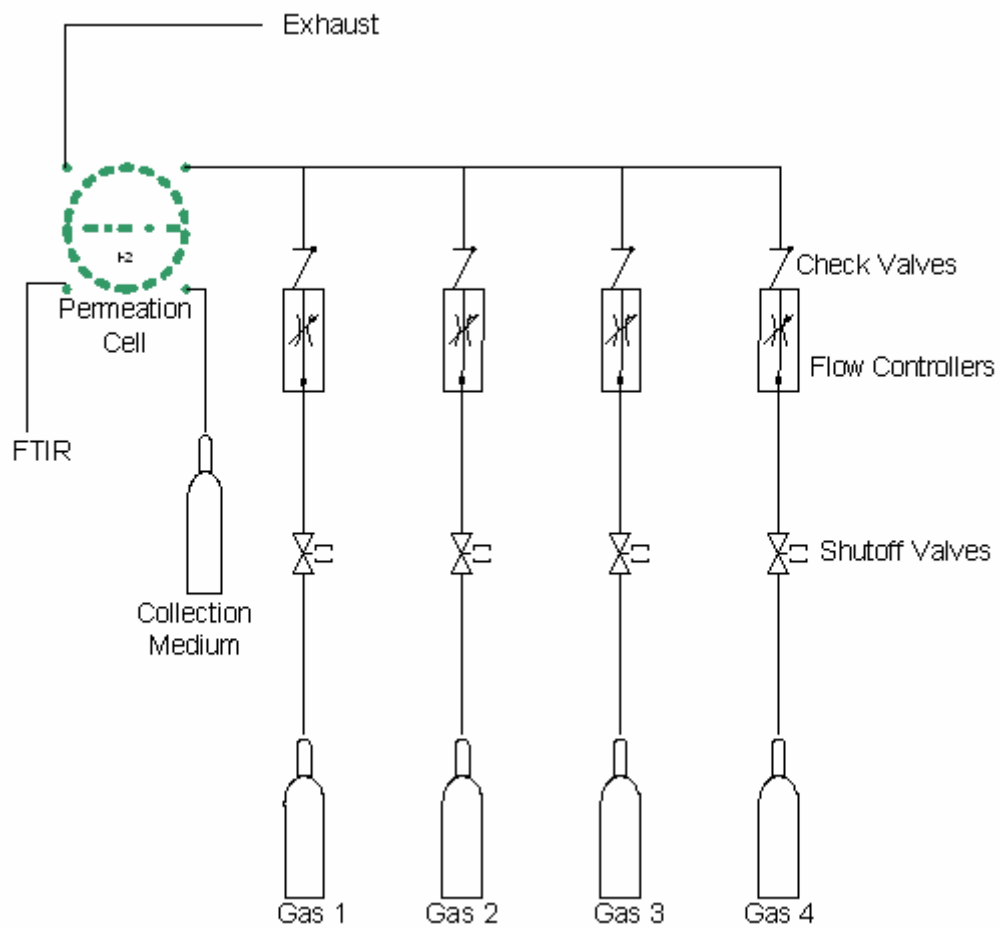


Figure 24: Schematic representation of proposed challenging gas mixing device.

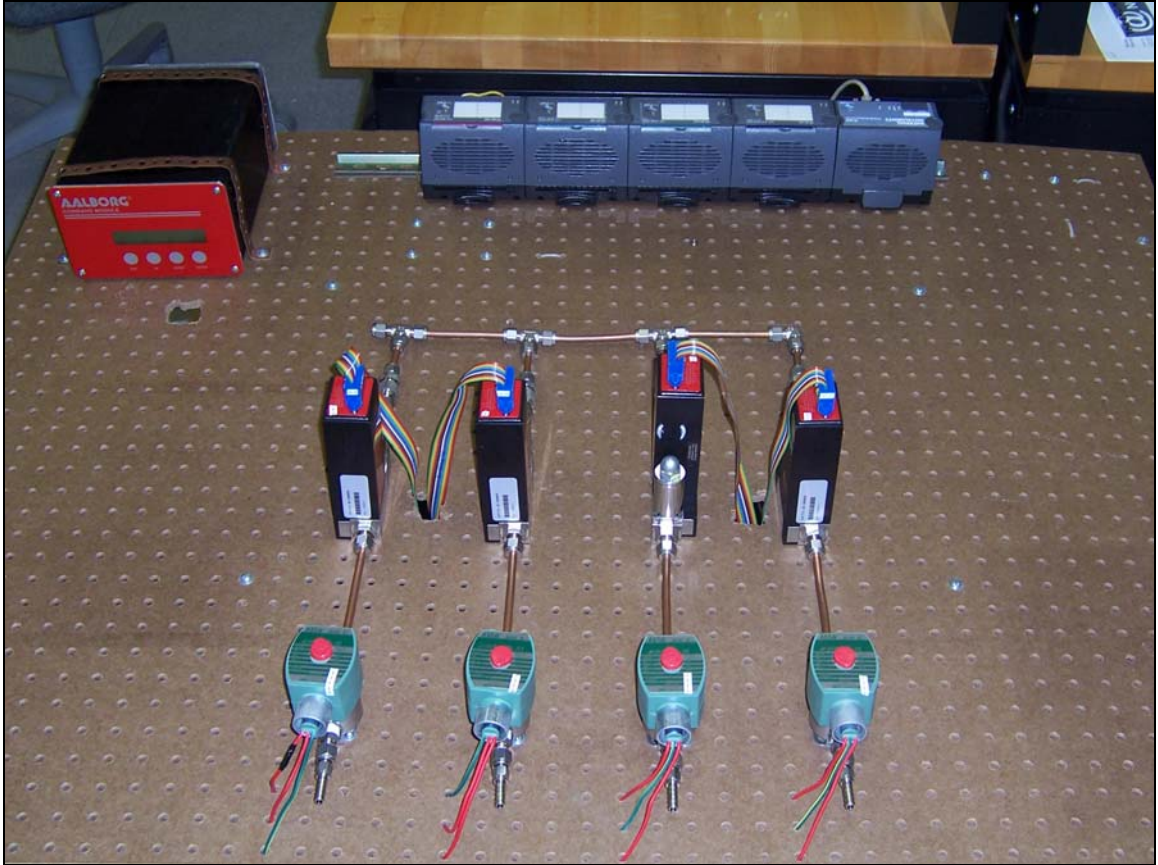


Figure 25: Gas mixing apparatus for creating mixed gaseous challenges for permeation testing.

The entire gas mixing system is wired through a National Instruments (Austin, TX) Fieldpoint[®] data acquisition system and controlled using LabView[®].

It is expected that these experiments will result in findings similar to those observed with various liquid mixtures. They may provide insight for modeling of multi-component gas permeation.

5.4 Combined Penetration/Permeation Test

A comprehensive study of all aspects of protection (i.e. penetration, sorption, and permeation) is rare but provides great insight for future testing needs. It was found that a combined penetration/permeation test could potentially prove quite valuable for future evaluations of chemical protective clothing materials.

The ASTM F903 method for penetration resistance specifies the application of pressure to drive a challenge agent through the material, whereas the ASTM F739 method for permeation resistance does not. The application of pressure in the F903 test is designed to replicate real-world use conditions (i.e. pressure applied in the fingertips of a glove when grasping, or pressure to a medical gown when leaning against a table). While these pressures are oftentimes intermittent and may affect penetration more heavily, they are certain to have at least some effect on permeation as well.

The author suggests designing a cell, shown conceptually in Figure 26, which would facilitate a combined test. Essentially, the test apparatus could consist of an F903 test assembly with a modified sample cell. The entire apparatus would be the same up to the membrane clamp. The ring clamp, which is open to the atmosphere, would be replaced. A replacement clamping device would be designed to simulate the collection

chamber of a typical F739 test cell. It would be completely sealed and would provide a mechanism for a collection medium (i.e. air or nitrogen) to be swept across the surface of the membrane. Any challenge agent that was driven (now on a molecular level) through the membrane by the applied pressure could be measured.

Such a system could potentially act as a universal test and make the ASTM F903 and ASTM F739 obsolete. Testing penetration and permeation in a single apparatus could solve one of the major challenges to this type of evaluation, cost. Additionally, this evaluation of permeation resistance with an applied pressure will provide a more representative view of how a chemical protective clothing material would perform in actual use.

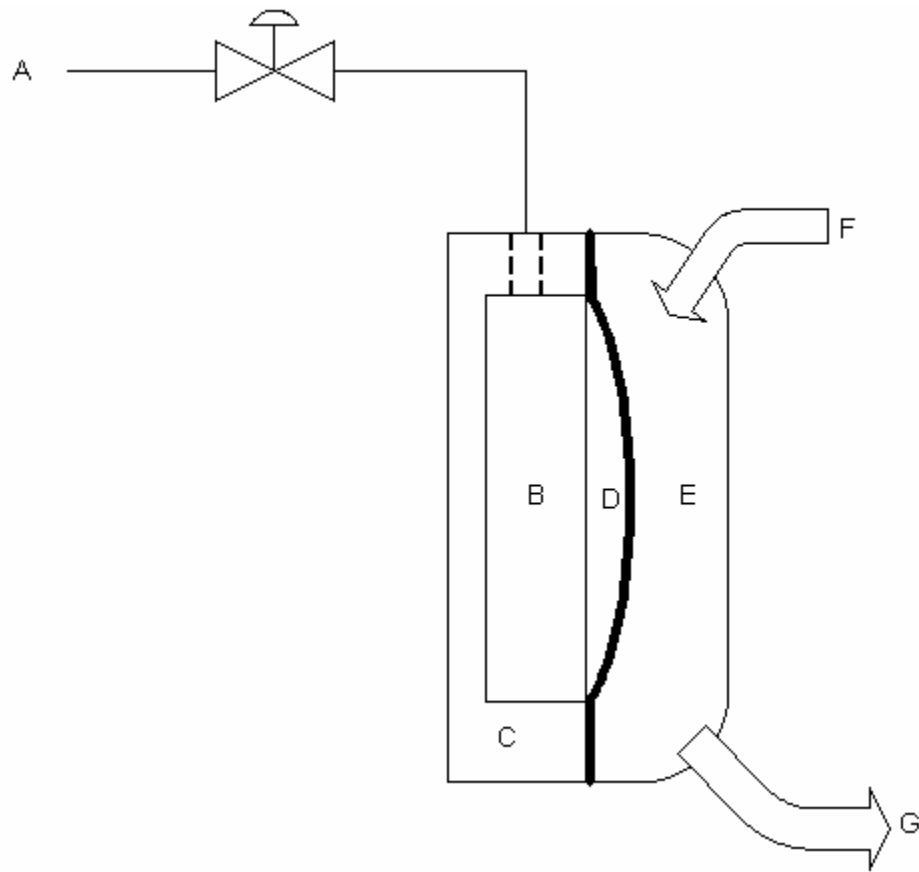


Figure 26: Schematic drawing of conceptual design for combination penetration/permeation test cell. Applied air pressure (A) will pressurize the challenge liquid (B), which is in the standard test cell body (C). This pressure will distend elastomeric polymer membranes (D). Any permeant released into the new collection chamber (E) will be picked up in the collection medium (F), which is being swept away to a detection device (G).

References

- [1] Walsh DL, Schwerin MR, Kisielewski RW, Kotz RM, Chaput MP, Varney GW, et al. 2004 Abrasion resistance of medical glove materials *Journal Of Biomedical Materials Research Part B-Applied Biomaterials* **68B** 81-87
- [2] Puri P, Hinestroza J, De Kee D 2005 Transport of small molecules through mechanically elongated polymeric membranes *Journal Of Applied Polymer Science* **96** 1200-1203
- [3] Hinestroza J, De Kee D, Pintauro PN 2001 Apparatus for studying the effect of mechanical deformation on the permeation of organics through polymeric films *Industrial & Engineering Chemistry Research* **40** 2183-2187
- [4] Aminabhavi TM, Munnolli RS, Stahl WM, Gangal SV 1993 Sorption And Diffusion Of Organic Esters Into Fluoropolymer Membranes *Journal Of Applied Polymer Science* **48** 857-865
- [5] Aminabhavi TM, Naik HG 1999 Sorption/desorption studies on polypropylene geomembrane in the presence of hazardous organic liquids *Journal Of Applied Polymer Science* **72** 1291-1298
- [6] Dixon-Garrett SV, Nagai K, Freeman BD 2000 Sorption, diffusion, and permeation of ethylbenzene in poly(1-trimethylsilyl-1-propyne) *Journal Of Polymer Science Part B-Polymer Physics* **38** 1078-1089
- [7] Hong SU, Barbari TA, Sloan JM 1997 Diffusion of methyl ethyl ketone in polyisobutylene: Comparison of spectroscopic and gravimetric techniques *Journal Of Polymer Science Part B-Polymer Physics* **35** 1261-1267
- [8] Ortego JD, Aminabhavi TM, Harlapur SF, Balundgi RH 1995 A Review Of Polymeric Geosynthetics Used In Hazardous-Waste Facilities *Journal Of Hazardous Materials* **42** 115-156
- [9] Li Y, De Kee D, Fong C, Pintauro P, Burczyk A 1999 Influence of external stress on the barrier properties of rubbers *Journal Of Applied Polymer Science* **74** 1584-1595

- [10] Xiao S, Moresoli C, Burczyk A, Pintauro P, De Kee D 1999 Transport of organic contaminants in geomembranes under stress *Journal Of Environmental Engineering-Asce* **125** 647-652
- [11] Xiao S, Moresoli C, Bovenkamp J, DeKee D 1997 Sorption and permeation of organic contaminants through high-density polyethylene geomembranes *Journal Of Applied Polymer Science* **65** 1833-1836
- [12] Hedlund J, Jareman F, Andersson C. Factors affecting the performance of MFI membranes. In: *Recent Advances In The Science And Technology Of Zeolites And Related Materials, Pts A - C*. Amsterdam: Elsevier Science Bv; 2004. p. 640-646.
- [13] Islam MA, Buschatz H 2005 Assessment of thickness-dependent gas permeability of polymer membranes *Indian Journal Of Chemical Technology* **12** 88-92
- [14] Valente AJM, Polishchuk AY, Burrows HD, Lobo VMM 2005 Permeation of water as a tool for characterizing the effect of solvent, film thickness and water solubility in cellulose acetate membranes *European Polymer Journal* **41** 275-281
- [15] Hansen CM 2004 Aspects of solubility, surfaces and diffusion in polymers *Progress In Organic Coatings* **51** 55-66
- [16] Van der Bruggen B, Jansen JC, Figoli A, Geens J, Van Baelen D, Drioli E, et al. 2004 Determination of parameters affecting transport in polymeric membranes: Parallels between pervaporation and nanofiltration *Journal Of Physical Chemistry B* **108** 13273-13279
- [17] ASTM 2004 F903-03 (2004) Standard Test Method for Resistance of Materials Used in Protective Clothing to Penetration by Liquids
- [18] Spurny KR 1991 Aerosol Penetration Through Protective Clothing *Journal Of Aerosol Science* **22** S789-S792
- [19] Shaw A, Cohen E, Hinz T 2004 Laboratory test methods to measure repellency, retention, and penetration of liquid pesticides through protective clothing Part II: Revision of three test methods *Textile Research Journal* **74** 684-688

- [20] Lankester BJA, Bartlett GE, Garneti N, Blom AW, Bowker KE, Bannister GC 2002 Direct measurement of bacterial penetration through surgical gowns: a new method *Journal Of Hospital Infection* **50** 281-285
- [21] Krzeminska S, Szczecinska K 2001 Proposal for a method for testing resistance of clothing and gloves to penetration by pesticides *Annals Of Agricultural And Environmental Medicine* **8** 145-150
- [22] Shaw A, Cohen E, Hinz T, Herzig B 2001 Laboratory test methods to measure repellency, retention, and penetration of liquid pesticides through protective clothing - Part I: Comparison of three test methods *Textile Research Journal* **71** 879-884
- [23] Kisielowski RW, Routson LB, Chaput MP, Lytle CD 2000 Modification of ASTM F 1671-97a, resistance of materials to penetration by blood-borne pathogens, for use with elastomeric materials *Journal Of Testing And Evaluation* **28** 136-138
- [24] Archibald BA, Solomon KR, Stephenson GR 1994 Fluorescent Tracer And Pesticide Penetration Through Selected Protective Clothing *Bulletin Of Environmental Contamination And Toxicology* **53** 479-485
- [25] Stull JO, White DF 1992 A Review Of Overall Integrity And Material Performance Tests For The Selection Of Chemical Protective Clothing *American Industrial Hygiene Association Journal* **53** 455-462
- [26] Sansone EB, Tewari YB 1978 Penetration Of Protective Clothing Materials By 1,2-Dibromo-3-Chloropropane, Ethylene Dibromide, And Acrylonitrile *American Industrial Hygiene Association Journal* **39** 921-927
- [27] Lee S, Obendorf SK 2001 A statistical model to predict pesticide penetration through nonwoven chemical protective fabrics *Textile Research Journal* **71** 1000-1009
- [28] Miller A, Schwartz P 2001 Forced flow percolation for modeling of liquid penetration of barrier materials *Journal Of The Textile Institute* **92** 53-62
- [29] Aminabhavi TM, Aithal US, Shukla SS 1988 An Overview Of The Theoretical-Models Used To Predict Transport Of Small Molecules Through Polymer Membranes *Journal Of Macromolecular Science-Reviews In Macromolecular Chemistry And Physics* **C28** 421-474

- [30] Neogi P 1996 Transport phenomena in polymer membranes *Plast. Eng.* **32** 173
- [31] Vrentas JS DJ 1986 Diffusion *Encycl. Polym. Sci. Eng.* **5** 36
- [32] Aminabhavi TM, Aithal US, Shukla SS 1989 Molecular-Transport Of Organic Liquids Through Polymer-Films *Journal Of Macromolecular Science-Reviews In Macromolecular Chemistry And Physics* **C29** 319-363
- [33] Vrentas JS, Vrentas CM 1998 Integral sorption in glassy polymers *Chemical Engineering Science* **53** 629-638
- [34] Ridge MC PJ 1989 Permeation of solvent mixtures through protective clothing elastomers *ASTM Spec. Tech. Publ.* **1037** 113
- [35] Crank J. *The Mathematics of Diffusion*. Second ed. New York: Oxford University Press; 1975.
- [36] Vrentas JS, Vrentas CM, Huang WJ 1997 Anticipation of anomalous effects in differential sorption experiments *Journal Of Applied Polymer Science* **64** 2007-2013
- [37] Neogi P 1983 Anomalous Diffusion Of Vapors Through Solid Polymers.1. Irreversible Thermodynamics Of Diffusion And Solution Processes *Aiche Journal* **29** 829-833
- [38] Alfrey J 1966 Diffusion in glassy polymers *Journal Of Polymer Science* **C12** 249
- [39] Sanopoulou M, Stamatialis DF, Petropoulos JH 2002 Investigation of case II diffusion behavior. 1. Theoretical studies based on the relaxation dependent solubility model *Macromolecules* **35** 1012-1020
- [40] Wolf CJ, Fu H 1996 Stress-enhanced transport of toluene in poly aryl ether ether ketone (PEEK) *Journal Of Polymer Science Part B-Polymer Physics* **34** 75-82
- [41] Ybarra RM, Neogi P, MacElroy JMD 1998 Osmotic stresses and wetting by polymer solutions *Industrial & Engineering Chemistry Research* **37** 427-434

- [42] Vrentas JS, Duda JL, Hsieh ST 1983 Thermodynamic Properties Of Some Amorphous Polymer Solvent Systems *Industrial & Engineering Chemistry Product Research And Development* **22** 326-330
- [43] Petropoulos JH, Sanopoulous M, Papadokostaki KG 1999 Fundamentals of transport phenomena in polymer solution-diffusion membranes *Surfactant Sci. Ser.* **79** 167
- [44] Vrentas JS, Vrentas CM 1993 Evaluation Of Free-Volume Theories For Solvent Self-Diffusion In Polymer Solvent Systems *Journal Of Polymer Science Part B-Polymer Physics* **31** 69-76
- [45] Cohen DS 1984 Diffusive Fronts Of Penetrants In Glassy-Polymers *Physica D* **12** 369-374
- [46] Cohen DS, Goodhart C 1987 Sorption Of A Finite Amount Of Swelling Solvent In A Glassy Polymer *Journal Of Polymer Science Part B-Polymer Physics* **25** 611-617
- [47] Durning CJ, Russel WB 1985 A Mathematical-Model For Diffusion With Induced Crystallization.2 *Polymer* **26** 131-140
- [48] Liu CPA, Nguyen DC, Neogi P 1990 Effects Of Constrained Chain Conformations On Polymer-Solute Interactions In Semicrystalline Polymers *Journal Of Macromolecular Science-Physics* **B29** 203-220
- [49] Durning CJ, Russel WB 1985 A Mathematical-Model For Diffusion With Induced Crystallization.1 *Polymer* **26** 119-130
- [50] Fong C, Moresoli C, Xiao S, Li Y, Bovenkamp J, De Kee D 1998 Modeling diffusion through geomembranes *Journal Of Applied Polymer Science* **67** 1885-1889
- [51] Crank J, Park GS, Editors. Diffusion in Polymers. New York: Academic Press; 1968.
- [52] Richman D, Long FA 1960 Measurement Of Concentration Gradients For Diffusion Of Vapors In Polymers *Journal Of The American Chemical Society* **82** 509-513

- [53] Long FA, Richman D 1960 Concentration Gradients For Diffusion Of Vapors In Glassy Polymers And Their Relation To Time Dependent Diffusion Phenomena *Journal Of The American Chemical Society* **82** 513-519
- [54] Petropoulos JH, Roussis PP 1978 Influence Of Transverse Differential Swelling Stresses On Kinetics Of Sorption Of Penetrants By Polymer Membranes *Journal Of Membrane Science* **3** 343-356
- [55] Thomas NL, Windle AH 1980 A Deformation Model For Case-II Diffusion *Polymer* **21** 613-619
- [56] Thomas N, Windle AH 1978 Transport Of Methanol In Poly(Methyl Methacrylate) *Polymer* **19** 255-265
- [57] Treloar LRG 1950 The Swelling Of Cross-Linked Amorphous Polymers Under Strain *Transactions Of The Faraday Society* **46** 783-789
- [58] Gee G, Stern J, Treloar LRG 1950 Volume Changes In The Stretching Of Vulcanized Natural Rubber *Transactions Of The Faraday Society* **46** 1101-1106
- [59] Wong TC, Broutman LJ 1985 Moisture Diffusion In Epoxy-Resins.1. Non-Fickian Sorption Processes *Polymer Engineering And Science* **25** 521-528
- [60] Wong TC, Broutman LJ 1985 Water In Epoxy-Resins.2. Diffusion Mechanism *Polymer Engineering And Science* **25** 529-534
- [61] Williams J 1974 Influence Of Drawing On Transport Properties Of Gases And Vapors In Polymers *Abstracts Of Papers Of The American Chemical Society* 67-67
- [62] Gent AN, Liu GL 1991 Diffusion Of Polymer-Molecules Into Polymer Networks - Effect Of Stresses And Constraints *Journal Of Polymer Science Part B-Polymer Physics* **29** 1313-1319
- [63] ASTM. Test Method F739-99a Standard Test Method for Resistance of Protective Clothing Materials to Permeation by Liquids or Gases Under Conditions of Continuous Contact. In.; 1999.

- [64] Anna DH, Zellers ET, Sulewski R 1998 ASTM F739 method for testing the permeation resistance of protective clothing materials: Critical analysis with proposed changes in procedure and test cell design *American Industrial Hygiene Association Journal* **59** 547-556
- [65] ASTM. E105-04 Standard Practice for Probability Sampling of Materials. In.; 2004.
- [66] Mansdorf SZ, Berardinelli SP 1988 Chemical Protective Clothing Standard Test Method Development.1. Penetration Test Method *American Industrial Hygiene Association Journal* **49** 21-25
- [67] Stull JO, White DF, Greimel TC 1992 A Comparison of the Liquid Penetration Test With other Chemical Resistance Tests and its Application in Determining the Performance of Protective Clothing *ASTM Spec. Tech. Publ.* **1133** 123-138
- [68] Wilusz E, Brennick JR, Gulliani DK, Hassler KD 1991 Novel barrier materials based on butyl rubber *Polym. Prepr. (Am. Chem. Soc., Div. Polym. Chem.)* **32** 296
- [69] Wilusz E, Hassler KD 1992 Chemical resistance properties of advanced glove materials *ASTM Spec. Tech. Publ.* **1133** 114
- [70] Schwoppe AD, Klein J, Sidman KR, Reid RC 1986 Sorption Desorption Phenomena Of Chemicals From Polymer (Paint) Films *Journal Of Hazardous Materials* **13** 353-367
- [71] Ehnthold DJ, Almeida RF, Beltis KJ, Cerundolo DL, Schwoppe AD, Whelan RH, et al. 1988 Test method development and evaluation of protective clothing items used in agricultural pesticide operations *ASTM Spec. Tech. Publ.* **989** 727
- [72] Pinette MFS, Stull JO, Dodgen CR, Morley MG 1992 A preliminary study of an intermittent collection procedure as an alternative permeation method for non-volatile, water insoluble chemicals *ASTM Spec. Tech. Publ.* **1133** 339
- [73] Park JK, Sakti JP, Hoopes JA 1996 Determination of volatile organic compound permeation through geomembranes *ASTM Spec. Tech. Publ.* **1261** 245
- [74] Prasad TV, Brown KW, Thomas JC 1994 Diffusion-Coefficients Of Organics In High-Density Polyethylene (Hdpe) *Waste Management & Research* **12** 61-71

- [75] Stampfer JF, McLeod MJ, Betts MR, Martinez AM, Berardinelli SP 1984 Permeation Of 11 Protective Garment Materials By 4 Organic-Solvents *American Industrial Hygiene Association Journal* **45** 642-654
- [76] Zellers ET, Sulewski R 1992 Glove permeation by propylene glycol monomethyl ether acetate - a photoresist solvent used in semiconductor device processing *Appl. Occup. Environ. Hyg.* **7** 392
- [77] Perron G, Banh TN, Pelletier L, Desnoyers JE, Lara J 2000 Volumetric and swelling techniques for studying the permeation of protective gloves to solvents *ASTM Spec. Tech. Publ.* **1386**
- [78] Aminabhavi TM, Harlapur SF, Aralaguppi MI 1997 A study on molecular transport of organic esters and aromatics into Viton fluoropolymers *Journal Of Applied Polymer Science* **66** 717-723
- [79] Mores M, Cassidy PE, Kerwick DJ, Koeck DC 1990 A review of polymer test methods applicable to geosynthetics for waste containment *ASTM Spec. Tech. Publ.* **1081** 12
- [80] Lee BL, Yang TW, Hassler KD, Wilusz E 1996 Effects of Biaxial Tensile Strain on Hydrocarbon Permeability of Butyl Rubber Composite Barriers *ASTM Spec. Tech. Publ.* **1237** 157-174
- [81] Haxo HE, Jr. 1990 Determining the transport through geomembranes of various permeants in different applications *ASTM Spec. Tech. Publ.* **1081** 75
- [82] Que Hee SS 1996 Simple glove permeation models *Appl. Occup. Environ. Hyg.* **11** 117
- [83] O'Callaghan K, Fredericks PM, Bromwich D 2001 Evaluation of chemical protective clothing by FT-IR/ATR spectroscopy *Applied Spectroscopy* **55** 555-562
- [84] August H, Tatzky R. Permeabilities of commercially available polymeric liners for hazardous landfill leachate organic constituents. In: Int. Conf. Geomembr.; 1984; 1984. p. 163.

- [85] Park JK, Sakti JP, Hoopes JA 1996 Transport of organic compounds in thermoplastic geomembranes.1. Mathematical model *Journal Of Environmental Engineering-Asce* **122** 800-806
- [86] Britton LN, Ashman RB, Aminabhavi TM, Cassidy PE 1989 Permeation And Diffusion Of Environmental-Pollutants Through Flexible Polymers *Journal Of Applied Polymer Science* **38** 227-236
- [87] Park JK, Nibras M 1993 Mass Flux Of Organic-Chemicals Through Polyethylene Geomembranes *Water Environment Research* **65** 227-237
- [88] Nelson GO, Priante SJ, Strong M, Anderson D, Fallon-Carine J 2000 Permeation of substituted silanes and siloxanes through selected gloves and protective clothing *Aihaj* **61** 709-714
- [89] Hinestroza J, De Kee D 2004 Permeation of organics through linear low density polyethylene geomembranes under mechanical deformation *Journal Of Environmental Engineering-Asce* **130** 1468-1474
- [90] Smith B. Infrared Spectral Interpretation: A Systematic Approach. New York: CRC Press; 1999.
- [91] Menard KP. Dynamic mechanical analysis: a practical introduction. Boca Raton, FL: CRC Press; 1999.
- [92] De Kee D, Fong C, Pintauro P, Hinestroza J, Yuan C, Burczyk A 2000 Effect of temperature and elongation on the liquid diffusion and permeation characteristics of natural rubber, nitrile rubber, and bromobutyl rubber *Journal Of Applied Polymer Science* **78** 1250-1255
- [93] Vrentas JS, Vrentas CM 1998 Temperature dependence of partition coefficients for polymer-solvent systems *Macromolecules* **31** 5539-5541
- [94] Aminabhavi TM, Phayde HTS 1995 Molecular-Transport Characteristics Of Santoprene Thermoplastic Rubber In The Presence Of Aliphatic Alkanes Over The Temperature Interval Of 25-Degrees-C To 70-Degrees-C *Polymer* **36** 1023-1033